

**IMPACT OF DYNAMIC AGEING ON THE FORMATION AND
STABILITY OF MODEL BILGE WATER OIL-IN-WATER EMULSIONS**

by

Rina Sabatello

A Thesis

Submitted to the Faculty of Purdue University

In Partial Fulfillment of the Requirements for the degree of

Master of Science in Materials Engineering



School of Materials Engineering

West Lafayette, Indiana

December 2021

THE PURDUE UNIVERSITY GRADUATE SCHOOL
STATEMENT OF COMMITTEE APPROVAL

Dr. Carlos J. Martinez, Chair

School of Materials Engineering

Dr. John A. Howarter, Chair

School of Materials Engineering

Dr. Kendra A. Erk

School of Materials Engineering

Approved by:

Dr. David Bahr

Dedicated to Mom, Dad, and Grandpa

ACKNOWLEDGMENTS

At the beginning of my sophomore year during my undergraduate career, I was paired with Professor Carlos Martinez as my academic advisor. Little did I know, he would become my mentor and my inspiration over the next few years. He offered me a position on his research team, encouraged me to travel across the country to present my research, and supported my decision to change my career path. I am endlessly grateful for the countless hours he has spent reviewing my papers and the time he has taken to help me become a better writer. In addition, the attention and care he has given to his students is unlike any other department and is something I will remember for the rest of my life. Next, I would like to thank my co-advisor, Professor John Howarter, and committee member Professor Kendra Erk for also encouraging me through my journey at Purdue. Thank you to the Strategic Environmental Research and Development Program (SERDP) for funding my research and giving me the opportunity to attend national conferences.

I cannot thank my graduate research mentor, Cole Davis, enough. He has helped me tremendously throughout my research with SERDP. I would also like to thank Brandon Wells, Yue Zheng, and Dr. Daniela Betancourt Jimenez for being outstanding team members in Professor Martinez's research group.

After living in West Lafayette for the past 6 years, I had the opportunity to engage with the community. I am forever thankful for Be Moved Power Yoga and Society Yoga for training me to become a yoga instructor, giving me an outlet to decompress, and allowing me to meet some of the most amazing men and women in Lafayette and West Lafayette. Some of which will be lifelong friends.

Lastly, I would like to thank my family. I am incredibly lucky to have two parents Rick and Tina, and a brother Antonio who supports all my endeavors and spends hours on the phone with me while at Purdue. In addition, I am grateful to have a close-knit extended family who always shows interest in my research. Lastly, I would like to acknowledge my boyfriend Jonathan and my two cats for being there for me in the most challenging times.

TABLE OF CONTENTS

LIST OF TABLES	7
LIST OF FIGURES	8
ABSTRACT	11
1. INTRODUCTION	13
1.1 Motivation and Challenges	13
1.2 Surfactant Chemistry	14
1.3 Emulsion Stability	15
1.4 Emulsion Ageing and Characterization	16
2. THE EFFECT OF DYNAMIC AGEING ON THE STABILITY OF OIL-WATER EMULSIONS WITH ANIONIC AND NONIONIC SURFACTANTS IN HIGH SALINITY WATER	18
2.1 Introduction	18
2.2 Materials and Methods	20
2.2.1 Emulsion Preparation	20
2.2.2 Emulsion Ageing Conditions	21
2.2.3 Emulsion Characterization	22
2.3 Results and Discussion	23
2.3.1 Impact of electrostatic charge on O/W emulsion stability	23
2.3.2 Effect of interfacial tension on O/W emulsion stability	25
2.3.3 Oil drop size after static ageing in salt	27
2.3.4 Oil drop size after dynamic ageing at 12 rpm	33
2.3.5 Oil drop size after dynamic ageing at 30 rpm	38
2.4 Conclusions	43
3. IMPACT OF LOW ENERGY MIXING ON THE STABILITY OF OIL-WATER EMULSIONS WITH ANIONIC AND NON-IONIC SURFACTANTS IN HIGH SALINITY WATER.	44
3.1 Introduction	44
3.2 Materials and Methods	45
3.2.1 Emulsion preparation	45

3.2.2	Emulsion ageing conditions and characterization	46
3.2.3	Energy density for dynamic ageing	46
3.3	Results and Discussion	47
3.3.1	Effect of dynamic ageing with 50% and 0% air inside the ageing vial	47
3.3.2	Effect of dynamic ageing on the dispersion of oil into surfactant and salt solutions	53
	Scenario 1: Dynamically ageing non-pre-mixed emulsions with 0% air	54
	Scenario 2: Dynamically ageing non-pre-mixed emulsions with 70% air	56
3.3.3	Surfactant-to-oil ratios that produce narrow drop size distributions	60
3.4	Conclusions	62
4.	CONCLUSIONS AND FUTURE PERSPECTIVES	64
4.1	Conclusions and Implications of Results	64
4.2	Future Perspectives	65
	APPENDIX A. SUPPORTING INFORMATION FROM CHAPTER 2	66
	REFERENCES	68
	VITA	74

LIST OF TABLES

Table 2.1: Values of CMC, surface excess concentration, and surfactant head group area for SLES and Triton X-100 in the presence of salt.....	27
Table 3.1: Emulsion compositions used to investigate unimodal drop distributions after dynamic ageing.....	61
Table 3.2: Light and heavy mineral oil density and viscosity at 40°C	61

LIST OF FIGURES

Figure 1.1: Chemical structures for a) SLES and b) Triton X-100.....	14
Figure 2.1: Photograph of a) the Benchmark BenchRocker 3D Nutating Shaker with tilt angle θ , and b) emulsification container with falling height h.	22
Figure 2.2: Zeta potential of emulsions with 5000 ppm mineral oil, 0.42 M NaCl, and 10 ppm - 2500 ppm SLES (black) and Triton X-100 (gray) after 3 hours of static ageing.	24
Figure 2.3: Optical microscopy of emulsions made with 5000 ppm Mineral Oil, 0.42 M NaCl, and 500 ppm of a) Triton X-100 and b) SLES after 3 hours of static ageing.....	24
Figure 2.4: Equilibrium interfacial tension of SLES + 0.42 M NaCl (black) and Triton X-100 + 0.42 M NaCl (gray) in mineral oil as a function of surfactant concentration. Equilibrium IFT was obtained via the Pendant Drop Method.	26
Figure 2.5: The evolution of average oil drop size distribution over 20 days for statically aged emulsions with a) SLES and b) Triton X-100 from 10 to 1000 ppm surfactant. The darkening of the distribution curves is proportional to time.	29
Figure 2.6: Average oil drop diameter, $D(4,3)$ during static ageing with increasing concentrations of SLES (left) and Triton X-100 (right). Lines were added between data points as visual guides. Dashed lines represent unstable emulsions that result from increased over time. Error bars represent the standard deviation.....	30
Figure 2.7: Photograph of the top view of a statically aged emulsion (20 days) with 0.42M NaCl, 10 ppm Triton X-100, and 5000 ppm mineral oil in a 50 mL centrifuge tube.	31
Figure 2.8: Photographs of (a) 500 ppm SLES, 0.42 M sodium chloride, and 5000 ppm mineral oil in a 50 mL centrifuge tube. The figure shows brightfield optical images of 500 ppm SLES, 0.42 M sodium chloride, and 5000 ppm mineral oil 20 days after emulsification.	31
Figure 2.9: The evolution of average oil drop size distribution over 20 days for dynamically aged emulsions with 70% air at 12 rpm with a) SLES and b) Triton X-100 from 10 to 1000 ppm surfactant. The darkening of the distribution curves is proportional to time.....	35
Figure 2.10: Brightfield optical image of 1000 ppm SLES aged for 20 days at 12 rpm.	36
Figure 2.11: Average oil drop diameter, $D(4,3)$ during dynamic ageing at 12rpm with 70% air and increasing surfactant concentration for SLES (left) and Triton X-100 (right). Dashed lines represent unstable emulsions that result from increased oil drop size over time. The darkening of the distribution curve is proportional to time.....	36
Figure 2.12: The evolution of average oil drop size distribution over 20 days for dynamically aged emulsions with 70% air at 30 rpm with a) SLES and b) Triton X-100 from 100 to 1000 ppm surfactant. The darkening of the distribution curves is proportional to time.....	39
Figure 2.13: Brightfield optical image of an emulsion (0.42M NaCl, 1000ppm SLES, 5000ppm mineral oil) dynamically aged at 30rpm for 20 days and with 70% air within the ageing vial....	39

Figure 2.14: Average oil drop diameter, $D(4,3)$ during dynamic ageing with 70% air at 30 rpm and increasing surfactant concentration for SLES (left) and Triton X-100 (right). Dashed lines represent unstable emulsions that result from increased oil drop size over time. The darkening of the lines is proportional to increased surfactant concentration.	40
Figure 2.15: Average oil drop size distribution after 20 days for 100 ppm SLES and 500 ppm Triton X-100 aged statically, dynamically at 12 rpm, and dynamically at 30 rpm.	42
Figure 3.1: Photographs of a 15 mL emulsion inside a) a 50 mL centrifuge tube with 70% air, b) a syringe with 50% air and c) a syringe with all air removed (0% air).	46
Figure 3.2: The evolution of average oil drop distribution over 20 days for dynamically aged emulsions with 50% air and concentrations from 10 – 1000 ppm of SLES. The darkening of the distribution curves is proportional to time.	48
Figure 3.3: Photograph of an emulsion dynamically aged for 5 days with 100 ppm SLES, 0.42 M sodium chloride, 5000 ppm mineral oil, and 0% air.	49
Figure 3.4: The evolution of average oil drop distribution over 20 days for dynamically aged emulsions with 0% air and concentrations from 10 – 1000 ppm of SLES. The darkening of the distribution curves is proportional to time.	51
Figure 3.5: Top view photograph of coalesced mineral oil drops in an emulsion with 10 ppm SLES, 0.42 M sodium chloride, and 5000 ppm mineral oil after 20 days of ageing with 0% air inside the syringe.	51
Figure 3.6: Brightfield optical images of a) 10 ppm b) 100 ppm c) 500 ppm and d) 1000 ppm SLES after 20 days of dynamic ageing with 0% air inside the syringe.	52
Figure 3.7: Photograph of the top view of a SLES and salt solution with 5000 ppm mineral oil added to the surface (0 days aged).	54
Figure 3.8: Photographs of the top view of emulsions with a) 10 ppm SLES and b) 1000 ppm SLES, 0.42 M sodium chloride, and 5000 ppm mineral oil that were not pre-emulsified and dynamically aged with 0% air for 10 days.	55
Figure 3.9: The average oil drop distribution for 10 – 1000 ppm of a) SLES and b) Triton X-100 after 10 days of dynamic ageing with 70% air. Mineral oil (5000 ppm) was dispensed, and the liquids were not pre-emulsified prior to ageing.	57
Figure 3.10: Brightfield optical images of a) 10 ppm and b) 1000 ppm SLES, 0.42 M sodium chloride, and 5000 ppm mineral oil after 10 days of dynamic ageing with 70% air and no pre-mixing.	57
Figure 3.11: Top view photographs of an emulsion with 1000 ppm SLES, 0.42 M sodium chloride, 5000 ppm Mineral oil after a) 0 days, b) 5 hours, and c) 2 days of dynamic ageing with 70% air and no pre-mixing.	58
Figure 3.12: Photograph of the top view of an emulsion with 100 ppm SLES, 0.42 M sodium chloride, and 5000 ppm mineral oil after 10 days of dynamic ageing with 70% air and no pre-mixing.	59

Figure 3.13: Optical Images of emulsions a) 2, b) 3, and c) 4 that were dynamically aged for 10 days at 30 rpm with 70% air within the ageing vial. The emulsions were made with heavy mineral oil and were not pre-mixed prior to ageing..... 62

Figure 3.14: Optical Images of emulsions a) 5, b) 6, and c) 7 dynamically aged for 10 days at 30 rpm with 70% air within the ageing vial. The emulsions were made with light mineral oil and were not pre-mixed prior to ageing. 62

ABSTRACT

Ships, including those in the US Navy, collect oily wastewater in their bilge due to onboard cleaning and mechanical operations. Oil-in-water emulsions (O/W) are present in bilgewater, and their filtration is difficult due to surfactants provided by cleaning products. Despite cleaning efforts, over 457,000 tons of oil are discharged into the ocean every year. An often overlooked aspect of bilgewater emulsions is their evolution, as the ship's movement at sea provides extra energy that can further emulsify the collected oil. This work aims to understand the effects of motion on model bilgewater emulsions by tracking their evolution in dynamic (rocking motion) and static conditions. The model bilgewater emulsion comprises mineral oil, deionized water with 0.42 M NaCl to mimic the salinity of seawater and sodium lauryl ether sulfate and Triton X-100, as commonly found anionic and nonionic surfactants, respectively. A rocker is used to simulate a ship motion; 15 mL of emulsion were placed in 50 mL centrifuge tubes to mimic partially filled bilgewater tanks. Emulsions were characterized via laser diffraction and optical microscopy. Model bilgewater emulsions with either SLES or Triton X-100 at concentrations above 100 ppm and 500 ppm, respectively, show long-term stability in static (no-rocking) conditions up to 20 days of observation. These concentrations represent the minimum surfactant concentration needed to obtain stable emulsions under static conditions. Under dynamic conditions, the minimum surfactant concentration to obtain stable emulsions increases to 500 ppm and 1000 ppm for SLES and Triton X-100, respectively. These results mean that the ship motion can induce drop coalescence in unstable emulsions with lower surfactant concentrations. However, the drop size distributions for stable emulsions under dynamic conditions show further emulsification as the average drop size decreases. The ship motion can help further reduce the size of the emulsion drops to diameters $< 2.8 \mu\text{m}$, which are significantly harder to filter out using current methods. A bilgewater tank partially filled will likely show a higher amount of sloshing than a filled one. To understand the effects of bilgewater storage volume on emulsification, a series of dynamic experiments were carried out with samples that contained up to 100% of the centrifuge tube volume occupied by the model bilge water emulsion. Even when 100% of the centrifuge volume is occupied and sloshing is eliminated, the oil moves due to density differences, and the shear stress between fluids can induce the generation of drops $< 2.8 \mu\text{m}$. In summary, this work shows that the ship motion provides enough energy for emulsification once a minimum surfactant

concentration is reached regardless of the volume of emulsion stored in the tanks. The data suggests that the best way to mitigate stable bilgewater emulsion formation is by reducing surfactant concentration.

1. INTRODUCTION

1.1 Motivation and Challenges

Ocean pollution resulting from land-based sources is well known. However, ocean pollution resulting from ocean-based sources is often overlooked. Ocean-based sources include the pollution of fishing ships, shipping vessels, cruise liners, and other ocean-going ships. Specifically, US Navy vessels have begun to investigate their contribution to oil pollution due to inefficient filtration of bilgewater. Bilgewater is a collection of liquids that is dispensed into a bilge tank as a result of waste produced from onboard cleaning procedures and mechanical operations. Bilgewater comprises fresh and seawater, oils from lubricants and engine fuels, surfactants from cleaning products, and particulates.¹⁻³ The liquids enter the bilge tank after being pumped through pipes. Once inside the bilge tank, oil is filtered from the bilgewater so that the remaining water can be safely ejected to the sea, and more wastewaters can be collected. The International Maritime Organization requires a concentration of less than 15 ppm of oil to be contained in the bilgewater before ejection.⁴ Despite filtration attempts, 457,000 tons of oil is ejected from ships every year.⁵

Oil is filtered from bilgewater through gravitational separation, chemical treatments, and other expensive techniques.^{2,3,6,7} However, even if these techniques were "successful," meaning 15 ppm of oil was measured in the bilgewater, small oil drops remain that are not detected. The accumulation of small, undetected oil drops that are ejected into the sea is a significant source of ocean pollution.^{3,8,9}

Oil drops incapable of being removed are stabilized by surfactants and form an oil-in-water (O/W) emulsion. The potential for emulsions to form begins onboard during cleaning operations. When oil is spilled, or equipment is cleaned, cleaning products containing surfactants remove the oil after scrubbing and agitation. The energy applied during scrubbing is sufficient to form O/W emulsions. Another source of emulsification occurs when the bilgewater is flushed down pipes before entering the bilge tank. Oil and water are sheared against the pipe walls, and the turbulent flow of the liquids promotes the breakup of oil in water. Lastly, a source of emulsification that goes unnoticed occurs once the bilgewater is collected. Whether a ship is at port or at sea, the motion of the waves causes

the ship to rock. This causes the bilgewater to slosh against the tank's walls and potentially provide enough energy to emulsify the oil further.

The main challenge of bilgewater is that the composition of compounds is unknown at any given time. Therefore, to effectively understand the fundamental behavior of bilgewater, a range of concentrations and types of bilgewater constituents must be studied. Nevertheless, gaining a fundamental understanding of the potential sources of bilgewater emulsification may provide solutions to prevent the formation of small oil drops and reduce the need for extensive filtration treatments.

1.2 Surfactant Chemistry

All cleaning products contain surfactants. Surfactants effectively remove oil and dirt from surfaces due to their ability to reduce the interfacial tension between oil and water.^{10, 11} The concentration of surfactants in bilgewater ranges from 10 – 2500 ppm and consist of anionic and non-ionic surfactants.^{6, 7, 12} **Figure 1.1** shows the chemical structure of common anionic surfactant sodium lauryl ether sulfate (SLES) and non-ionic surfactant Triton X-100. Anionic surfactants have a negatively charged, hydrophilic head group whose properties are affected by salt in the aqueous phase. On the other hand, the properties of non-ionic surfactants are not heavily influenced by salt due to their uncharged head group.

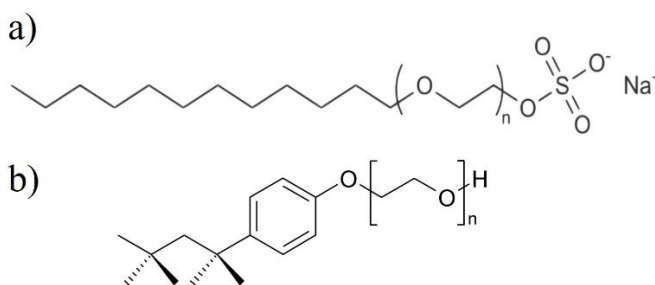


Figure 1.1: Chemical structures for a) SLES and b) Triton X-100.

When added to a mixture of oil and water, surfactants align at the oil/water interface and reduce the interfacial energy. Upon the addition of energy via scrubbing or agitation, oil is broken up into drops of various sizes.¹³ The size of the oil drops depends on the energy added, the oil volume

fraction, the interfacial tension, and the surfactant concentration. If added in sufficient concentrations, surfactants cover the newly formed interface and provide a physical barrier around the oil drops. The strength barrier formed by the surfactant head groups is dependent on the chemistry and interaction between head groups. For non-ionic surfactants, the head group forms hydrogen bonds with water and is affected by steric hindrance.¹⁴ For anionic surfactants, counterions present in solution form an electrostatic double-layer that screens the negative charge on the anionic surfactant. As the salt concentration in the solution increases, the double-layer shrinks, the electrostatic repulsion between headgroups is reduced, and more anionic surfactants can pack at the interface.^{15, 16} The salt concentration in seawater contains 0.42 M sodium chloride (NaCl).⁵ The presence of salt in bilgewater directly affects the properties of anionic surfactants and their ability to stabilize O/W emulsions.

1.3 Emulsion Stability

Stable emulsions are unfavorable in bilgewater. Most emulsions are kinetically stable due to the adsorption of surfactants, meaning the chemical and physical properties of an emulsion do not change with time.^{14–17} For bilgewater, stability is defined as emulsions with oil drop that are too small to be filtered and whose size does not change over time. Therefore, unstable bilgewater emulsions are favored, as oil is easily removed.

An emulsion can undergo various mechanisms to become unstable over time¹. For example, gravitational separation occurs when the dispersed phase either creams to the surface or sediments depending on the density of the dispersed phase. For hydrocarbon-based oils, the density is less than water, so oil drops experience creaming above a given size. Onboard, it was estimated that oil droplets less than 20 μm are difficult to remove after gravitational separation techniques have been executed.^{3, 18} However, this is an overestimate according to Peclet number calculations. The Peclet number describes the ratio of buoyancy forces and Brownian motion. A Peclet number ≥ 1 will result in oil drops that cream to the surface, and a Peclet number < 1 describes oil droplets dispersed in solution and dominated by Brownian motion.¹⁹ The Peclet diameter is defined as the oil droplet size to which buoyancy forces overcome Brownian motion. A simple calculation of the Peclet diameter can be found in Equation 1.1:

$$d_{Pe} = \left[\frac{(Pe)6k_B T}{\pi \Delta \rho g} \right]^{1/4} \quad (1.1)$$

where P_e is the Peclet number, k_B is the Boltzmann constant, T is temperature, $\Delta \rho$ is the difference in density between the oil and water, and g is the acceleration due to gravity.²⁰ From this calculation, mineral oil droplets (density = 0.82 g/mL) larger than 2.8 μm in diameter are predicted to be dominated by buoyancy resulting in creaming.

Next, flocculation occurs when two or more drops are attracted to each other through van der Waals forces, but the individual drop size is unaffected.¹ When oil drops are flocculated, the van der Waals attractive forces are more significant than long-range electrostatic repulsion. As the previous section states, the electric double layer surrounding oil drops and electrostatic repulsion decrease as salt concentration increases. Therefore, oil drops in bilgewater systems are susceptible to flocculation.²¹ Flocculated oil drops cream faster than single oil drops due to a larger effective diameter and stronger buoyancy force for flocculated drops.¹⁷

Lastly, an emulsion becomes unstable if drops undergo coalescence. Two drops merge and form one larger drop to reduce the interfacial area between oil and water and reduce the system's free energy. If the surfactant concentration is insufficient to cover the interfacial area between oil and water, oil drops can coalesce until the interface is saturated. However, the energy due to electrostatic repulsion and steric hindrance provided by surfactants must be overcome when oil drops coalesce. Oil drops can coalesce upon collision, during gravitational separation, or during flocculation. Like flocculated aggregates, a coalesced oil drop creams faster than two separate smaller drops.^{1, 22}

Overall, any destabilization mechanism to induce gravitational separation or increase the rate of gravitational separation is favored in bilgewater filtration applications.

1.4 Emulsion Ageing and Characterization

To study the long-term stability of emulsions, the oil drop size and distribution is measured over time. The storage of emulsions is referred to as ageing. If the drop size increases during ageing

(due to coalescence or flocculation), the emulsion is unstable. To effectively characterize the stability of an emulsion, the evolution of the oil drop distribution must be considered in addition to the average oil drop size. Bilgewater emulsions contain a wide range of oil drop sizes. Therefore, a reliable technique to measure the entire drop distribution of model bilgewater emulsions is required.

The most common technique to characterize oil drop size and distribution is through optical microscopy. However, this technique is limited by the resolution of the microscope. For example, drops below 1 μm are not accurately imaged nor measured due to Brownian motion.^{22, 23} To overcome this, laser diffraction is employed to effectively measure oil drops ranging from 0.01 to 3000 μm in diameter.^{1, 24} During laser diffraction, an aliquot of an emulsion is diluted and exposed to a laser beam to which oil drops scatter the light. The scattering pattern, or the intensity and angle at which a drop scatters light, depends on the drop size.^{1, 22, 25} Mie theory is a mathematical model used in instrument software that relates the scattering pattern to the size distribution based on the oil properties. The software produces a plot of oil concentration (volume) as a function of drop diameter based on the best fit distribution between the Mie theory and measured scattering pattern.¹

Static ageing refers to the storage of emulsions under static conditions. Long-term stability for statically aged O/W emulsions with common anionic and non-ionic surfactants has been established in the literature.^{26–29} Under static conditions, oil drops large enough to overcome Brownian motion will experience instability by means explained in section 1.3.

In food and cosmetic industries, model O/W emulsions are statically aged to mimic the long-term behavior of a product on a shelf. In contrast, ships do not experience static behavior due to rocking influenced by waves. Therefore, dynamic ageing refers to the storage of emulsions under motion provided by external mechanical energy.

2. THE EFFECT OF DYNAMIC AGEING ON THE STABILITY OF OIL-WATER EMULSIONS WITH ANIONIC & NONIONIC SURFACTANTS IN HIGH SALINITY WATER

2.1 Introduction

Ships, including those in the US Navy, collect oily wastewater in their bilge due to onboard cleaning and mechanical operations. The time it takes before bilgewater is eventually treated and discharged varies on each vessel depending on maritime conditions and whether the ship is at port or sea. Oil-in-water emulsions (O/W) are present in bilgewater, and their filtration is difficult due to surfactants provided by cleaning products, which disperse oil in the water. Bilgewater must contain less than 15 ppm of oil⁵ before releasing it into the ocean. Despite cleaning efforts, over 457,000 tons of oil are discharged into the ocean every year.⁵ The potential for emulsions to form in vessels begins in routine cleaning procedures onboard, such as surface cleaning, laundry, and personal care. During these procedures, cleaning products containing surfactants are used to remove compounds onboard like hydrocarbons (e.g., engine oil, diesel fuel, and lubricants) and particulates.^{1, 2} During cleaning operations, scrubbing and agitation can aid in the formation of O/W emulsions. The liquids and compounds are pumped through a series of pipes and tanks before collection in the bilge. The turbulent flow and shear of the fluids inside the pipe also can generate O/W emulsions. Once collected, the bilgewater is stored in the bilge tank before it is treated. An often overlooked aspect of bilgewater emulsions is their evolution, as the ship's movement at sea provides extra energy that can further emulsify the collected oil. This work aims to understand the effects of motion on model bilgewater emulsions by tracking their evolution in dynamic (rocking motion) and static conditions.

One challenge with bilgewater emulsions is that the composition and concentration of oils, surfactants, and any particulate matter is unknown at any given time. In general, bilgewater contains a mixture of ionic and non-ionic surfactants whose concentrations range from 10 to 2500 ppm.^{6, 7, 12} Cleaning products utilize ionic and non-ionic surfactants because they effectively lower the interfacial tension between oil and water.^{10, 11} When surfactants are present in a mixture of oil and water under turbulent flow, the added energy causes the oil to break up and form a distribution of dispersed oil drop sizes.¹³ The oil drop size distribution depends on the interfacial tension and

viscosity between the oil and aqueous phases, oil volume fraction, energy density input, and surfactant concentration present in the emulsion. Depending on the type of surfactant, if an emulsion is formed with a sufficient surfactant concentration, the resulting oil drops have the potential to be stable for days or months.^{10, 11, 26, 27, 30, 31} For bilgewater, the goal is to remove as much oil as possible by destabilizing the emulsion.

Emulsions can become unstable due to flocculation, gravitational separation (sedimentation or creaming), and coalescence.¹ Unstable emulsions are favored in bilgewater so that oil can be easily removed. Onboard, the large oil drops formed due to creaming, flocculation, and coalescence are removed via skimming. Hydrocarbon-based oils are less dense than water, so depending on the size of the drop, the oil will cream to the surface. The Peclet number describes the ratio of buoyancy forces and Brownian motion size at which oil drops overcome Brownian motion in the Peclet diameter. For example, drops with diameters $< 1 \mu\text{m}$ are dominated by thermal energy (Brownian motion) and remain dispersed for relatively long periods.³² For mineral oil, the estimated Peclet diameter is about $2.8 \mu\text{m}$ (Equation 1.1). Additional techniques are required for the removal of these oil drops^{2, 3, 6, 7}, but are not completely successful and the oil drops are not detected nor removed.

When the liquids are stored inside the tank before the oil is filtered, the simple rocking of the ship imposes energy that may lead to emulsion formation. The storage or ageing of emulsions under static conditions with common anionic and non-ionic surfactants has been studied throughout the literature.^{27–29} Attempts to accelerate static ageing of O/W emulsions include centrifugation which uses a centrifugal force to destabilize an emulsion due to creaming.^{1, 33} However, limitations for this method exist because the centrifugal force is greater than the force of gravity and would not be observed during static storage conditions.¹ Therefore, changes in oil drop size distribution generated by accelerated ageing tests must be compared to those generated after static storage. Efforts to destabilize O/W emulsions have utilized agitation tanks with impellers at various mixing speeds to induce coalescence.^{34, 35} The resulting oil drop size distribution and the frequency of coalescence produced by mechanical agitation depend on impeller speed, impeller dimensions, mixing time, and composition of emulsion.^{26, 34, 35} Although these studies have provided critical results about the effect of surfactant concentration, type, and ageing on emulsion stability, the

effect of ship motion on bilgewater emulsion stability must be investigated due to the non-static storage conditions onboard.

The impact of ship motion on the stability of model bilgewater emulsions with anionic and non-ionic surfactants has not been studied in the literature. Any process during storage, such as sloshing of liquids that produces sub-micron drops, is unfavorable to bilgewater filtration. In this work, model emulsions were dynamically aged to mimic the storage of bilgewater on a ship at sea. Model emulsions were composed of anionic or non-ionic surfactant concentrations between 10 and 1000 ppm with fixed concentrations of 0.42 M sodium chloride to resemble the concentration of seawater⁵, and a fixed concentration of 5000 ppm mineral oil to represent engine lubricants. The liquids were emulsified in a centrifuge tube and stored under static and dynamic conditions for 20 days. Static ageing provides a baseline for the minimum surfactant concentration required to form stable emulsions. This condition would also mimic the behavior of a ship at port. The behavior of a ship exposed to ocean waves was modeled by placing the emulsions on a three-dimensional rocker at two different speeds. Mineral oil drop size measurements were conducted via laser diffraction and optical microscopy after 0, 5, 10, and 20 days to determine emulsion stability. The evolution of oil drop size distributions during dynamic ageing was compared to the drop size distributions during static ageing to investigate the effects of ship rocking on the generation of sub-micron oil drops. Understanding the chemical and physical behaviors of the emulsions found in bilgewater is relevant to reducing ocean pollution and potentially reducing the cost of current filtration systems by preventing the formation of stable emulsions. These results will expand on existing knowledge of bilgewater and potentially lead to strategies for cleaning bilgewater that reduce ocean pollution.

2.2 Materials and Methods

2.2.1 Emulsion Preparation

Model bilgewater emulsions were prepared in 50 mL centrifuge tubes. Non-ionic surfactant, Triton X-100 (Sigma- Aldrich, Laboratory-grade, $M_w = 625$ g/mol), or anionic surfactant, sodium lauryl ether sulfate (SLES) (STEOL US-170UB, Stepan Co., $M_w = 332.4$ g/mol), were used in the preparation of O/W emulsions at concentrations of 10, 100, 500, and 1000 ppm. The continuous

phase consists of 0.42 M sodium chloride (Sigma-Aldrich), and the dispersed phase consists of 5000 ppm heavy mineral oil (Sigma-Aldrich) for a total emulsion volume of 15 mL. Consequently, about 70% of air existed within the centrifuge tube. Emulsions in this chapter are referred to emulsions with 70% air. Onboard, it was estimated that oil drops less than 20 μm are difficult to remove after physical separation techniques have been executed.^{3, 18} Therefore, before ageing, the emulsions were mixed in a VWR (VDI 25) high shear mixer at 24,000 rpm for 1 minute (energy density of 162 J/mL, see Appendix A for calculation) to form an average oil drop size of 20 μm .

2.2.2 Emulsion Ageing Conditions

Emulsions were both statically and dynamically aged. Static ageing refers to the storage of emulsions without external motion. Dynamic ageing was used to replicate the motion of a ship at sea. Ship oscillations at sea vary but can be approximated by a frequency of 10.8 cycles per minute.³⁶ A 3-dimensional rocker (Benchmark BenchRocker 3D Nutating Shaker), shown in **Figure 2.1**, was used to emulate ship movement. After 20 days, this provided the emulsions with an additional energy density input of 8.8 J/mL. This value is an upper-end estimate and arises from the balance between a falling object's potential and kinetic energy and can be viewed in the Appendix A. Since the oscillation rate and amplitude of ship rocking depend on maritime conditions, the rocker speed was varied from 12 and 30 rpm to represent low and high oscillation frequencies of ship motion. Prior to ageing, the emulsions were prepared using a rotor-stator mixer to form a target oil drop size of 20 μm , as stated in the previous section.

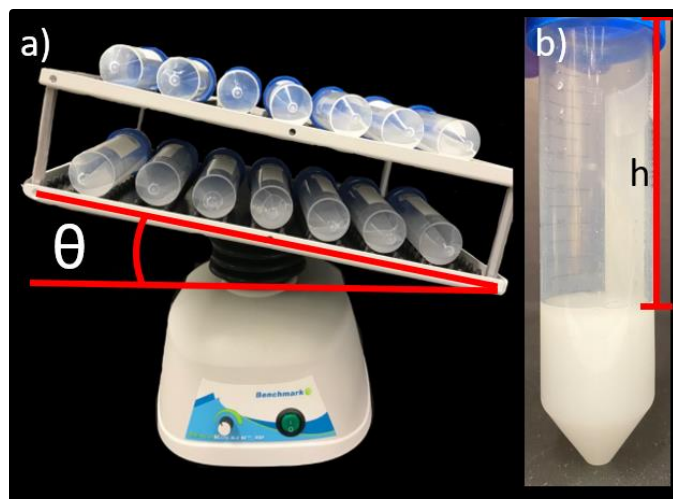


Figure 2.1: Photograph of a) the Benchmark BenchRocker 3D Nutating Shaker with tilt angle θ , and b) emulsification container with falling height h .

2.2.3 Emulsion Characterization

To determine the electrostatic stability of emulsions with respect to surfactant chemistry, the zeta potential of emulsion drops was measured (Malvern Zetasizer Nano ZS) with 10 – 2500 ppm SLES or Triton X-100. All emulsions tested contained 0.42 M NaCl. Measurements were made 3 hours after initial emulsification under static storage conditions.

The interfacial tension between surfactant solutions and heavy mineral oil was measured (RameHart Goniometer) via Pendant Drop Method at concentrations of 0.001 – 10 mM of SLES or Triton X-100. Aqueous surfactant solutions contained 0.42 M NaCl and were dispensed through a needle submerged in mineral oil. Drops were equilibrated for at least 60 minutes or until the interfacial tension value (measured every 30 seconds) remained constant over time. The average equilibrium IFT was calculated from three separate drops. The critical micelle concentration (CMC) was determined from the resulting interfacial tension isotherms.

The stability of model bilgewater emulsions was determined by measuring oil drop size at 3 hours, 5, 10, and 20 days after emulsification using laser diffraction (Malvern Mastersizer 3000). Initial oil drop size measurements began at 3 hours to ensure removal of air bubbles generated upon high shear mixing of the emulsions. A drop size distribution was measured using laser diffraction measurements. Laser diffraction calculates a volume average oil drop size distribution and a

volume-weighted mean drop diameter, presented as $D(4,3)$.²⁴ Each size distribution was measured 5 times to produce an average drop size distribution. All emulsion formulations studied were prepared in triplicate, and the reported oil drop size distributions are an average of those three measurements. An aliquot of the emulsions was collected in glass capillaries after gently swirling the bulk emulsion to ensure proper sampling. The prepared glass capillaries were imaged using an Olympus BX41 microscope with the AM Scope software.

2.3 Results and Discussion

2.3.1 Impact of electrostatic charge on O/W emulsion stability

Anionic and non-ionic surfactants can stabilize oil in water emulsions at different concentrations due to the electrostatic charge at the oil-water-surfactant interface. The magnitude of the charge at the oil/water interface depends on the type of the surfactant^{15–17, 37, 38} and impacts the distance at which oil drops can approach each other. The zeta potential of emulsions made with 5000 ppm mineral oil and 0.42 M NaCl was measured over a range of surfactant concentrations (10 ppm – 2500 ppm). These experiments establish a baseline for the stability of the emulsions based on surfactant type and concentration under static conditions. **Figure 2.2** shows the zeta potential for SLES and Triton X-100 emulsions after 3 hours of statically ageing. An electrostatic double-layer exists around the drops that consist of counterions in solution and provides a screening effect. The double-layer shrinks as the salt concentration increases and drops interact at shorter distances before experiencing electrostatic repulsion.^{15, 16} For example, at a salt concentration of 0.42 M NaCl, the Debye length, or the distance at which the electrostatic effects are prevalent, is approximately 0.47 nm. This distance can be compared to the Bjerrum length, or the distance at which the electrostatic interaction between two charged drops is comparable to thermal energy, which is 0.71 nm in room temperature deionized water.³⁹

It is known that without the addition of surfactants and salt, the charge at the oil-water interface is negative due to the adsorption of hydroxide ions that exist in water.⁴⁰ The results in **Figure 2.2** show that for the non-ionic surfactant, 100 ppm of Triton X-100 reduced the zeta potential. This is due to limited adsorption of hydroxide ions onto the O/W interface due to the energetically favorable adsorption of the neutral surfactant onto the oil drops.³⁷ **Figure 2.3** shows optical

microscopy images of emulsions with 500 ppm Triton X-100 and 0.42 M NaCl that were statically aged for 3 hours. **Figure 2.2** shows that oil drops around 200 μm were flocculated, resulting from zeta potential values close to zero. The addition of salt greater than 0.1 M produced signs of instability such as flocculation and coalescence for non-ionic surfactant emulsions.³⁸

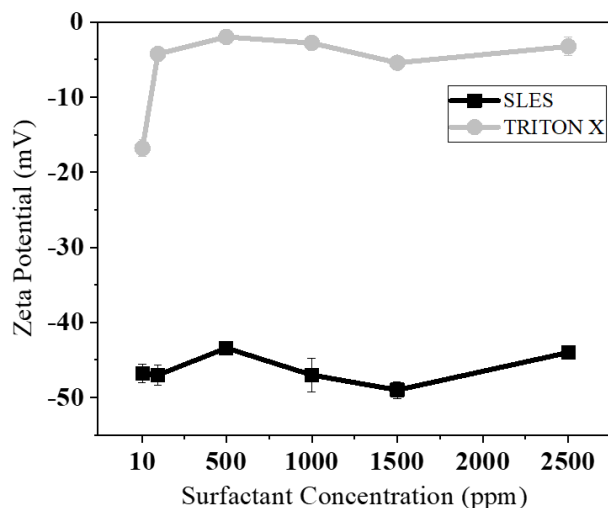


Figure 2.2: Zeta potential of emulsions with 5000 ppm mineral oil, 0.42 M NaCl, and 10 ppm - 2500 ppm SLES (black) and Triton X-100 (gray) after 3 hours of static ageing.

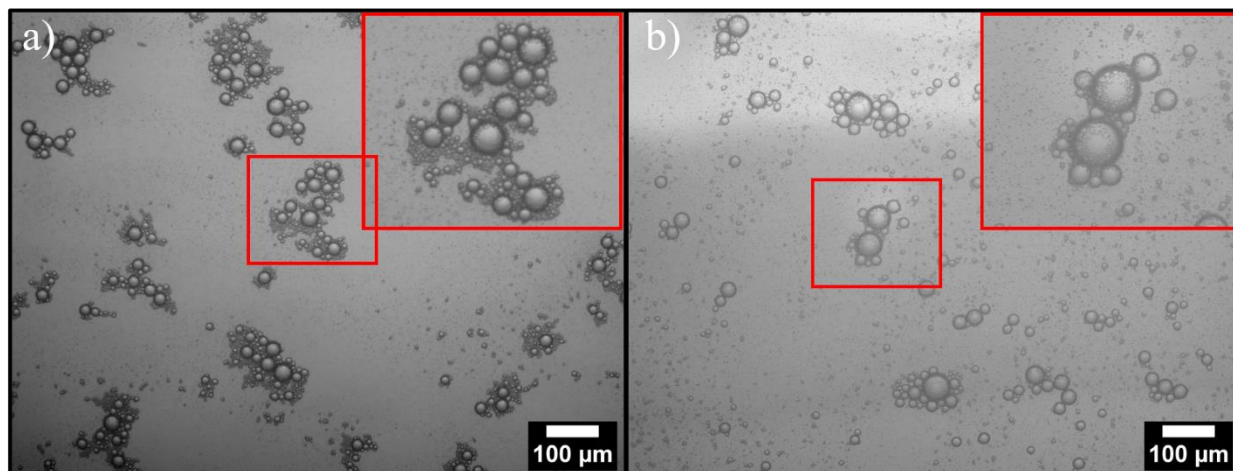


Figure 2.3: Optical microscopy of emulsions made with 5000 ppm Mineral Oil, 0.42 M NaCl, and 500 ppm of a) Triton X-100 and b) SLES after 3 hours of static ageing.

Emulsions prepared with SLES showed a greater magnitude of zeta potential compared to emulsions with Triton X-100. As anionic surfactants adsorb to oil drops, the zeta potential becomes more negative and increases in magnitude compared to surfactant-free oil drops in water.¹⁵ As the anionic surfactant-covered oil drops approach each other, the repulsion between the drops is greater than oil drops with non-ionic surfactants due to the charged head group on the surfactant.¹⁶ As a result, the degree of flocculation due to van der Waals forces for emulsions with anionic surfactant is less than that of emulsions with a non-ionic surfactant. The optical image in **Figure 2.3b** shows that with 500 ppm SLES (concentration above the CMC), many of the smallest visible oil drops remain singularly dispersed, and there is less oil in large flocs than the drops in **Figure 2.3a**. The implications of these results are discussed in the proceeding sections.

2.3.2 Effect of interfacial tension on O/W emulsion stability

The addition of surfactants to an oil-in-water emulsion reduces the interfacial tension (IFT) between the two phases and lowers the energy needed for emulsification.⁴¹ Obtaining the IFT with respect to surfactant concentration aids in the determination of the critical micelle concentration (CMC), the surface concentration (Γ_s), and the surfactant head group area (\AA). The CMC is the concentration at which surfactants can align into a configuration with the lowest surface energy. Below this concentration, there is not enough surfactant to effectively cover the oil/water interface and therefore, the emulsion is unstable due to coalescence.⁴² The surface concentration (Γ_s), is the concentration of surfactant that forms a monolayer around an oil drop and is inversely proportional to the surfactant head area. Therefore, as the surfactant head group area is reduced, the surface concentration increases due to efficient surfactant packing at the interface, and the IFT is reduced.⁴³ The resulting oil drop size is not only dependent on the total surfactant concentration but also the surfactant-to-oil ratio (S/O).^{17, 31, 44} For example, oil in water emulsions did not form if the S/O is below a critical threshold of 0.1.¹⁷ However, this threshold is not universal and depends on salt concentration, energy added during emulsion generation, and surfactant type.

Figure 2.4 displays the equilibrium IFT, γ , between mineral oil and SLES, and mineral oil and Triton X-100, both in aqueous 0.42 M NaCl. Two regimes were present within the IFT isotherms: where the IFT is dependent on surfactant concentration and a regime where the IFT is constant with surfactant concentration. After performing a linear regression on the two regimes, the CMC

was calculated from the intersection of the two fitted lines. The slope of the data points within the first regime was steeper for SLES than Triton X-100. The value of each slope was used in Equation 2.2^{30, 46} to determine the concentration of surfactant per area at the surface (Γ_s). The value of n depends on the number of adsorbed species (surfactants and/or counterions) onto the interface.^{30, 47, 48} For the system with a non-ionic surfactant or anionic surfactant in the presence of salt, the value of n is 1.^{49, 50} An additional estimation of the amount of each surfactant (C_a) needed to form monodisperse drops (d) at a given oil volume fraction (Φ) was calculated using Equation 3.¹ **Table 2.1** summarizes the calculated surfactant characteristics based on the IFT measurements. According to **Table 2.1**, SLES has a greater surface concentration and smaller head group area, which can pack more densely at the oil-water interface than with Triton X-100.

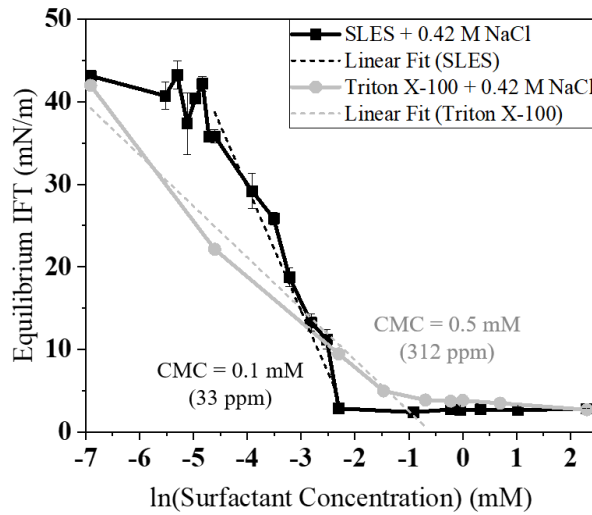


Figure 2.4: Equilibrium interfacial tension of SLES + 0.42 M NaCl (black) and Triton X-100 + 0.42 M NaCl (gray) in mineral oil as a function of surfactant concentration. Equilibrium IFT was obtained via the Pendant Drop Method.

$$\Gamma_s = \frac{-1}{nRT} * \frac{\partial \gamma}{\partial \ln(C_a)} \quad (2.2)$$

$$C_a = \frac{6\Gamma_s\phi}{d} \quad (2.3)$$

Table 2.1: Values of CMC, surface excess concentration, and surfactant head group area for SLES and Triton X-100 in the presence of salt.

Surfactant Type	CMC with 0.42M NaCl [ppm]	Surface Concentration, Γ_s [$10^{-6} \text{ mol}/\text{m}^2$]	C_a Needed to form 1 μm monodisperse drops [ppm]	Surfactant Head Area, A [$\text{\AA}^2/\text{molecule}$]
SLES	33	6.05	70	27.4
Triton X-100	312	2.51	55	66.2

In a salt-free environment, previous studies found the CMC and surface excess concentration were 324 ppm and $2.43 \times 10^{-6} \text{ mol}/\text{m}^2$, respectively for Triton X-100³⁰, and agrees with the data in **Table 2.1**. In other published experiments, the CMC for salt-free emulsions with SLES was between 233 ppm⁵¹ and 288 ppm.⁵² Therefore, we can expect the CMC to be less than 233 ppm in the presence of salt, which agrees with the data in **Table 2.1**. Previously established by Kedar and Bhagwat, the addition of 0.17 M NaCl reduced the IFT of SLES and crude oil to 3 mN/m. The surface concentration calculated was approximately $2 \times 10^{-6} \text{ mol}/\text{m}^2$.⁴⁸ Thus, we can expect an increase in the surface concentration for SLES with increasing salt concentration, as more anionic surfactant molecules can pack at the oil/water interface. This assumption is verified by the data in **Table 2.1**, which shows that the surface concentration for SLES is $6.05 \times 10^{-6} \text{ mol}/\text{m}^2$ with the addition of 0.42 M NaCl. The following sections discuss the stability against coalescence of mineral oil-in-water emulsions concerning the effects of electrostatic charge and interfacial tension.

2.3.3 Oil drop size after static ageing in salt

Emulsions aged under static conditions were used as a control for the stability of model bilgewater emulsions. Surfactant type and concentration were varied to explore the range of surfactant chemistries and concentrations present in bilgewater. **Figure 2.5a** and **Figure 2.5b** present the average oil drop size distributions of statically aged emulsions with 10 to 1000 ppm of SLES and Triton X-100, respectively, and were measured at 0 days (3 hours), 5, 10, and 20 days. In **Figure 2.5a**, emulsions with < 10 ppm SLES were unstable, shown by a shift in the drop size distribution

at 0-days. For example, within 10 days, the initial peak at 5-6 μm shifted towards 40 μm , and a new peak at 2 mm was formed. This behavior contributed to an overall increase in $D(4,3)$ over time. At 10 ppm SLES, a concentration below the CMC (~ 30 ppm), there was not enough surfactant to form stable emulsions, and coalescence occurred. As the concentration of SLES increased to 100 ppm, the distribution did not change between 5 and 20 days and was stable against coalescence. According to **Table 2.1**, about 30 ppm SLES is needed to form 1 μm monodisperse oil drops, so it can be expected that 100 ppm SLES is sufficient to produce an emulsion stable to coalescence. Between 0 and 5 days for 100 ppm SLES, there was an increase in volume % of 20 μm oil drops and a decrease in volume % for 2 μm oil drops due to coalescence of the smaller oil drops as the emulsion attempts to reach equilibrium. There is significant excess surfactant for concentrations ≥ 500 ppm SLES, and the emulsion remained stable over time.

The CMC is larger in emulsions with Triton X-100, meaning more surfactant is required to stabilize Triton X-100 emulsions. **Figure 2.5b** shows that emulsions prepared with $\leq \sim 300$ ppm Triton X-100 exhibited a shift in the distribution similar to emulsions with 10 ppm SLES (**Figure 2.5a**) and indicate that coalescence has occurred. Emulsions with ≥ 500 ppm Triton X-100 were stable against coalescence between 0 and 20 days, as there was more than enough surfactant to stabilize the drops.

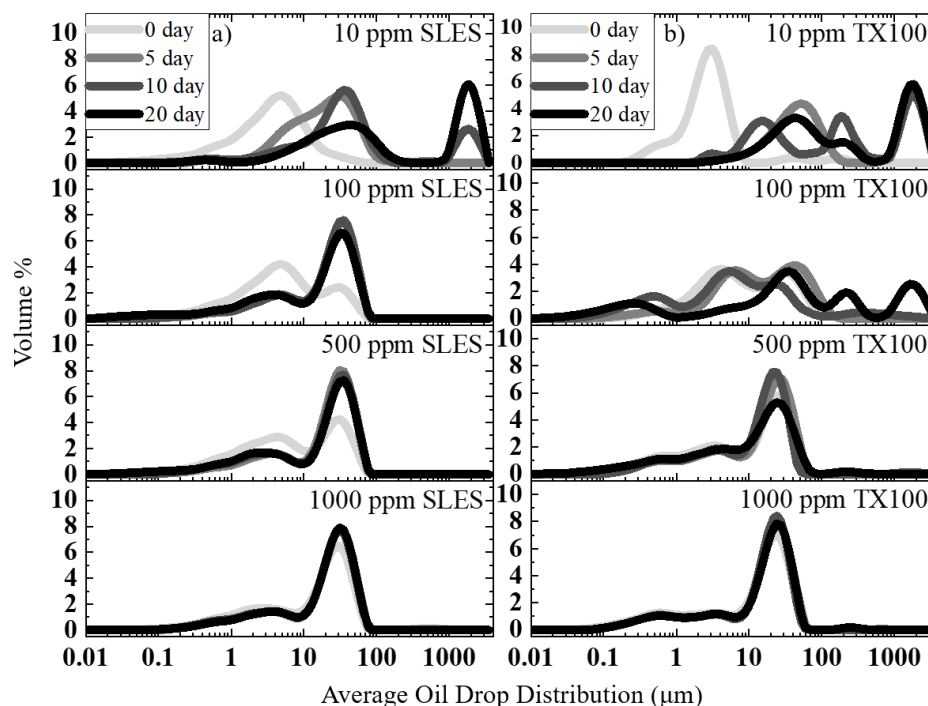


Figure 2.5: The evolution of average oil drop size distribution over 20 days for statically aged emulsions with a) SLES and b) Triton X-100 from 10 to 1000 ppm surfactant. The darkening of the distribution curves is proportional to time.

Figure 2.6 summarizes the results presented in **Figure 2.5** by plotting the $D(4,3)$ over 20 days for all SLES and Triton X-100 concentrations. Three hours after emulsification (0 days on the chart), the average oil drop sizes for all surfactant concentrations and chemistries were between 5 μm and 30 μm in diameter. For SLES emulsions, the $D(4,3)$ increased over time for concentrations ≤ 10 ppm due to coalescence but did not change significantly for concentrations ≥ 100 ppm. The average oil drop diameter after 20 days with 1000 ppm SLES was 25 μm . For Triton X-100 emulsions, the $D(4,3)$ increased within 20 days for concentrations ≤ 100 ppm due to coalescence but was constant for concentrations ≥ 500 ppm. The oil drop diameter after 20 days for 1000 ppm Triton X-100 was 22 μm . During static ageing, the minimum surfactant concentration to form stable emulsions is 100 ppm, or 0.30 mM SLES and 500 ppm, or 0.80 mM Triton X-100 for emulsions made with 5000 ppm mineral oil. In this case, it takes less SLES to form stable emulsions during static ageing.

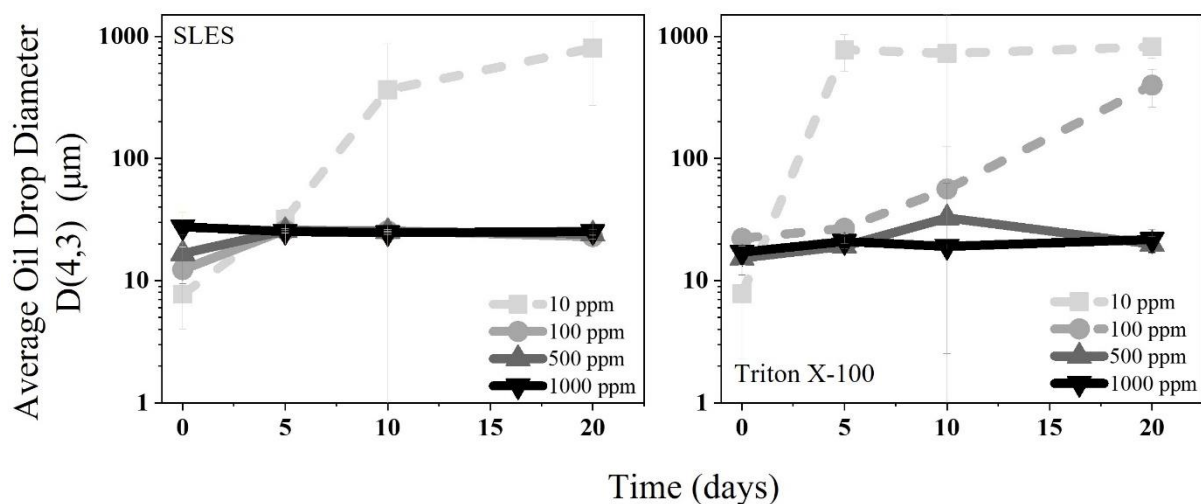


Figure 2.6: Average oil drop diameter, $D(4,3)$ during static ageing with increasing concentrations of SLES (left) and Triton X-100 (right). Lines were added between data points as visual guides. Dashed lines represent unstable emulsions that result from increased over time. Error bars represent the standard deviation.

Visual observations verified the coalescence of oil drops in emulsions made with 10 ppm – 100 ppm of surfactant. **Figure 2.7** shows optical images of the surface of an emulsion with 10 ppm Triton X-100 aged statically for 20 days. Millimeter-sized oil drops that were not present after the initial emulsification were formed due to coalescence and creaming. Coalescence was not observed in emulsions with ≥ 500 ppm of either surfactant. **Figure 2.8** presents optical micrographs of an emulsion with 500 ppm SLES after 20 days of static ageing. The vials were gently swirled before sampling to ensure the optical micrographs represented the bulk emulsion. Drops approximately 50 μm in diameter were not included in the initial drop size distribution but existed at the surface of the emulsion as a result of creaming; however, these emulsions were considered stable because they did not undergo coalescence to cause an increase in overall $D(4,3)$.

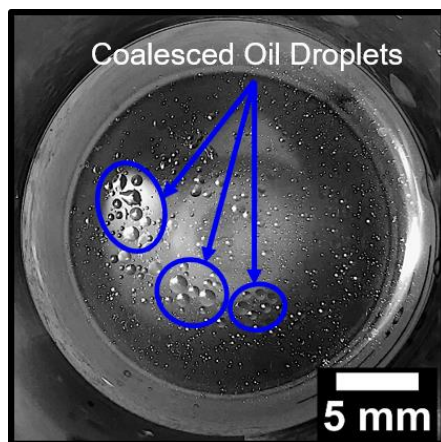


Figure 2.7: Photograph of the top view of a statically aged emulsion (20 days) with 0.42M NaCl, 10 ppm Triton X-100, and 5000 ppm mineral oil in a 50 mL centrifuge tube.

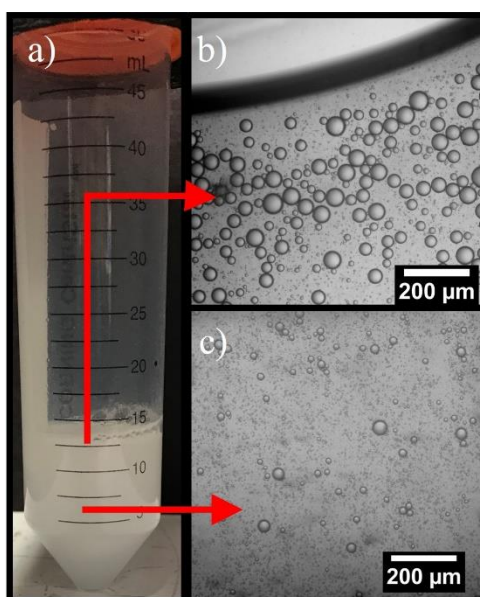


Figure 2.8: Photographs of (a) 500 ppm SLES, 0.42 M sodium chloride, and 5000 ppm mineral oil in a 50 mL centrifuge tube. The figure shows brightfield optical images of 500 ppm SLES, 0.42 M sodium chloride, and 5000 ppm mineral oil 20 days after emulsification.

According to the oil drop size distributions and D(4,3) plots in **Figure 2.5** and **Figure 2.6**, the minimum concentration is required to form an emulsion with little change in oil drop size distribution over time is greater for Triton X-100 than SLES. This is because SLES had a greater magnitude of zeta potential than Triton X-100 in the presence of salt. The adsorption of charged molecules onto an oil/water interface increased as NaCl was added and, in turn, increased the magnitude of the zeta potential.¹⁵ Oil in water emulsions stabilized by anionic surfactants obtained zeta potential values as low as -60 mV in the presence of NaCl,¹⁷ which coincide with the zeta potential values for SLES in **Figure 2.2**. The stability of the oil drops was due to the adsorption of charged surfactants and subsequent repulsion between oil drops. From visual observations in **Figure 2.3**, oil drops covered in SLES experienced more repulsion than oil drops covered in Triton X-100. Larger zeta potential values lead to repulsion that decreased the coalescence rate of oil drops at high surfactant concentration and constant ionic strength (0.01 M NaCl).⁵³

During emulsification, the initial oil drop sizes are dependent on the amount of energy used to make the emulsion, the surfactant concentration and type⁴⁵, the interfacial tension⁴¹, and the surfactant-to-oil ratio.¹⁷ Assuming the high-energy input for this system remains constant at 24,000 rpm for 1 minute, and the oil volume fraction was constant at 0.0058, the oil drop distribution is contingent on the properties provided by the surfactant. After emulsifying oil and water at high input energy, small oil drops are formed, which causes an increase in the total interfacial area.¹⁷ If the surfactant concentration is low enough, the oil drops coalesce until the surfactant can efficiently cover the oil drops.^{30, 54} As a result, the interfacial tension decreases as the surfactant concentration increases up to the CMC.^{43, 52, 55} Beyond this concentration, an excess amount of surfactant provides sufficient coverage of oil drops and stabilizes them against coalescence.^{45, 56} The resulting average oil drop size depends on surfactant type. For example, previous work showed that without salt, anionic surfactants formed smaller oil drops than non-ionic surfactants when the S/O was greater than 0.03.⁵⁷ Therefore, at any surfactant above its CMC, it is expected to see the average oil drop size reach a value independent of surfactant concentration.

For each surfactant tested, the surfactant concentration threshold to form stable emulsions is also dependent on the surface concentration. For example, in **Section 2.3.2**, SLES had a greater surface concentration than Triton X-100, meaning more SLES was at the oil/water interface than Triton

X-100. The results from static ageing indicate stable emulsions were present at a S/O of 0.02 for SLES. Stable emulsions with Triton X-100 existed at a S/O of 0.1. Therefore, at a constant oil volume fraction, less SLES is required for stable emulsions. The general trend is vital in bilgewater applications because the surfactant concentration can vary significantly.^{30, 32}

As mentioned previously, the estimated Peclet diameter for mineral oil drops is about 2.8 μm . The oil drop size distributions in **Figure 2.5** show that most of the distributions are composed of drops with diameters larger than 2.8 μm and will cream due to gravity. Therefore, static ageing conditions. However, ships at sea are not static, and ship motion can easily redisperse creamed oil drops. Therefore, it is necessary to investigate how the stability threshold changes when emulsions are subjected to movement during ageing.

2.3.4 Oil drop size after dynamic ageing at 12 rpm

The previous section established a foundation for the effect of surfactant concentration and type on the stability of statically aged emulsions. In addition, a threshold for the minimum concentration of each surfactant needed to form stable emulsions was determined. The purpose of observing O/W emulsions under dynamic storage conditions is to provide insight into the effects of ship movement or other low-energy events on the stability of model bilgewater emulsions. After initial emulsification, the samples were stored on a three-dimensional gyrating rocker at 12 and 30 rpm to mimic shipboard movement, and contained 70% air within the ageing vials.

Figure 2.9 shows the oil drop size distributions for dynamically aged emulsions at 12 rpm for up to 20 days with 70% air. Emulsions made with 10 ppm of either surfactant exhibit similar behavior to emulsions of the same composition in **Figure 2.5** that were aged statically. As the concentration of SLES increased to 100 ppm, two additional peaks appeared in the distribution at 2 mm and 0.5 μm . The peak at 2 mm for 100 ppm is lower than the peak at 2 mm formed at 10 ppm SLES; however, the peak at 0.5 μm indicates that small drops are formed due to the energy provided by rocking at 12 rpm. The formation of small drops can be explained by the effective change in the capillary number, which is a ratio of fluid velocity and interfacial tension, where large capillary numbers indicate a dominant inertial force.⁴³ Compared to static ageing, dynamic ageing at 12 rpm introduced a greater fluid velocity, which indicates an increased capillary number. For systems

with large capillary numbers, oil drop diameters decreased due to the deformation and breakup of oil.⁵⁸ This process is likely a combination of rapid drop breakup and relatively slower coalescence of the subsequent small drops. At 500 ppm SLES, the initial peak at 40 μm decreased, and an additional peak at 0.5 μm formed within 5 days of ageing due to the breakup of drops. However, after 10 days of ageing, the peak at 0.5 μm decreased, and the peak at 40 μm increased, suggesting that subsequent coalescence has occurred. Although this emulsion did not produce oil drops 2 mm in diameter, the distribution at 20 days resulted from coalescence and drop breakup. Finally, at 1000 ppm SLES, drop breakup is dominant within the first 5 days of ageing as the initial peak around 30 μm shifts toward 2 μm . By 10 days, a peak around 40 μm formed, indicating coalescence. After 20 days, this peak shifted toward 50 μm and the peak at 2 μm continued to shift towards 0.5 μm . An optical micrograph of this emulsion is presented in **Figure 2.10**, where drops $\leq 50 \mu\text{m}$ exist. When an emulsion is mixed in a high shear mixer, the oil drop size is produced due to the competition between coalescence and oil drop breakup. Even though dynamic ageing at 12 rpm provides minimal energy compared to high shear mixing, the evolution of emulsion drop size also competes between coalescence and drop breakup.

The behavior for Triton X-100 emulsions is similar to that of SLES emulsions. At 10 ppm, there is a clear indicator for coalescence as the 0-day peak at 1.5 μm shifts to 20 μm , and a second peak at 2 mm was formed. As mentioned earlier, at this concentration of Triton X-100, there is not enough surfactant to effectively cover the interface of oil drops and prevent coalescence. At 100 and 500 ppm Triton X-100, there are indications for both coalescence and drop breakup. The results of static ageing in Section 3 determined that 100 ppm was not enough to stabilize oil drops, so coalescence is expected. As shown in **Table 2.1**, 55 ppm of Triton X-100 was needed to form 1 μm monodisperse drops, so the small peak at 0.5 μm is expected due to the energy provided rocker. At 500 ppm Triton X-100, signs of coalescence did not occur until after 10 days as the 2 mm peak was not present at 0 or 5 days of dynamic ageing. Because 500 ppm Triton X-100 is above the CMC and the energy input was > 0 for dynamic ageing, a peak at 0.5 μm appeared at 5 days, indicating drop breakup. However, the height of the peak decreased after 20 days of ageing, which denotes coalescence. As with SLES, there is a competition between drop breakup and coalescence during dynamic ageing at 12 rpm. At 1000 ppm Triton X-100 there is more than enough surfactant to stabilize the emulsion. Drop breakup is evident as the initial peak at 20 μm

shifts to 0.4 μm after 20 days. The shift in distribution toward smaller oil drop sizes provides evidence of further emulsification.

Overall, at a surfactant concentration of ≥ 100 ppm for either surfactant, rocking at 12 rpm produced more oil drops ≤ 1 μm in diameter than after initial emulsification. These oil drops are smaller than the Peclet diameter and are disadvantageous to oil separation in bilgewater, as they are dominated by Brownian motion rather than gravity.

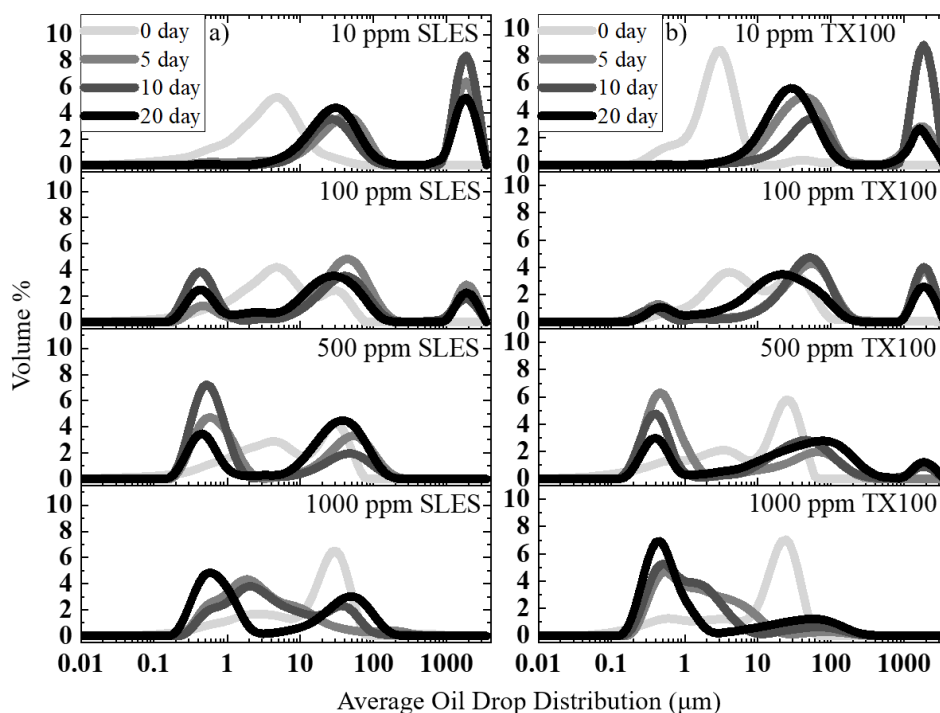


Figure 2.9: The evolution of average oil drop size distribution over 20 days for dynamically aged emulsions with 70% air at 12 rpm with a) SLES and b) Triton X-100 from 10 to 1000 ppm surfactant. The darkening of the distribution curves is proportional to time.

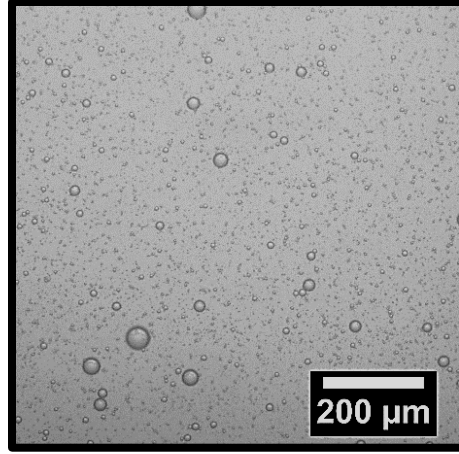


Figure 2.10: Brightfield optical image of 1000 ppm SLES aged for 20 days at 12 rpm.

A summary of the average oil drop diameters during dynamic ageing at 12 rpm is shown in **Figure 2.11**. **Figure 2.11a** displays an increase in $D(4,3)$ for emulsions with 10 and 100 ppm SLES between 0 and 5 days. **Figure 2.11b** shows that the $D(4,3)$ increases within 5 days for emulsions with 10, 100, and 500 ppm of Triton X-100 due to coalescence. However, both drop breakup and coalescence occurred for ≤ 100 ppm SLES and ≤ 500 ppm Triton X-100, coalescence was dominant and produced an overall increase in $D(4,3)$ within 5 days. This threshold differs from static ageing due to the energy imparted by the rocker.

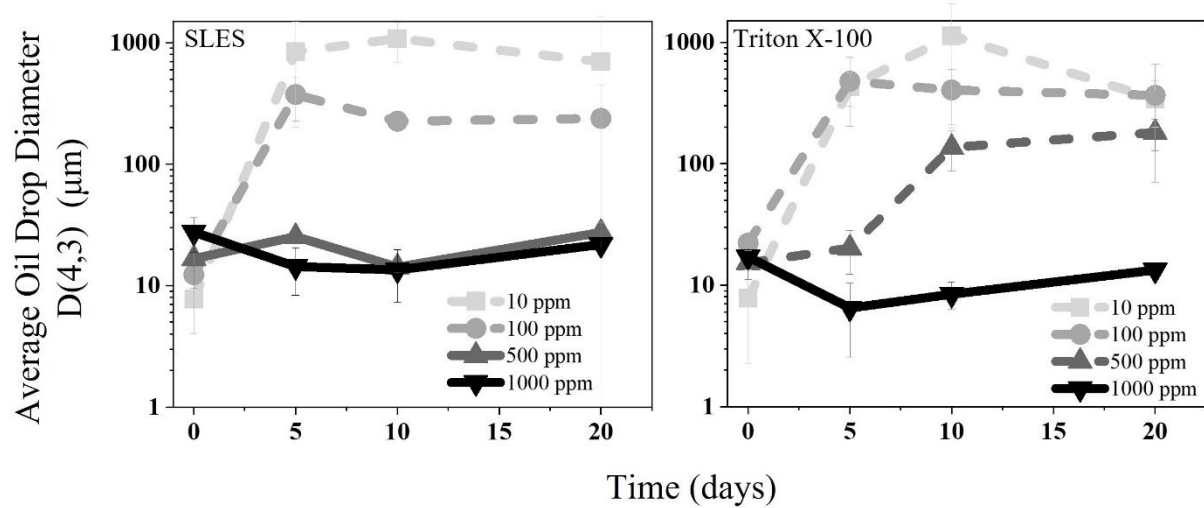


Figure 2.11: Average oil drop diameter, $D(4,3)$ during dynamic ageing at 12rpm with 70% air and increasing surfactant concentration for SLES (left) and Triton X-100 (right). Dashed lines represent unstable emulsions that result from increased oil drop size over time. The darkening of the distribution curve is proportional to time.

According to these results, the threshold of emulsion stability against coalescence was increased compared to static ageing. The S/O ratio required to form stable emulsions during dynamic ageing at 12 rpm is 0.1 for SLES and 0.2 for Triton X-100. Previously stated in **Section 2.3.1**, the electrostatic repulsion between oil drops with Triton X-100 was less than the repulsion between oil drops with SLES and existed in a more flocculated state, as seen in **Figure 2.3**. However, these flocs were easily broken up if disturbed. During dynamic ageing, the emulsion is in motion, and the flocs are broken, but the electrostatic charge on the oil drops should not change. Drops covered in non-ionic surfactants exist closer than oil drops covered in anionic surfactants due to their increased steric repulsion brought on by anionic surfactants.^{16, 17} Therefore, oil drops with Triton X-100 have a greater probability of colliding and coalescing than oil drops with SLES. This explains the increase in the stability threshold between the different surfactant types.

The increase in stability threshold between surfactant concentrations can be explained through the available interfacial area for surfactant adsorption. Below the stability threshold, dynamic ageing at 12 rpm causes oil drops to coalesce and influence a larger average drop size. At a larger average drop size, there is less interfacial area for SLES or Triton X-100 to adsorb to the oil/water interface. Therefore, fewer smaller drops were produced, and there was not enough surfactant to efficiently cover the surface of oil drops, and instability to coalescence was observed.^{30, 54}

Oil spill remediation attempts to add dispersants to the ocean's surface to lower the interfacial tension between the floating oil and water to form dispersed oil drops.^{31, 44} This process reduces the amount of oil at the ocean's surface due to oil spills and benefits animals and other marine life that frequent the ocean surface. The effectiveness of the dispersants was studied by Li et al., who utilized a wave tank simulator to replicate the motion of waves at sea: crashing waves and calm, non-crashing waves. It was found that the dispersion effectiveness depends on how much energy was produced by the wave. For the case of calm waves, little energy was provided, and large oil drops greater than 200 μm in diameter were produced without the presence of surfactants, and smaller drops were present at greater depths with surfactants.³¹ Similarly, at a S/O ratio of 0.04, sub-micron drops existed in the presence of turbulent motion.⁴⁴ This information supports the results in this paper by proving that the energy provided by waves is enough to generate emulsions.

The usage of the rocker at 12 rpm was intended to mimic normal sea conditions. The amount of energy provided at 12 rpm was enough energy to break large oil drops and induce coalescence. A ship at sea is subjected to not only calm waters but also storms, larger waves, or other sources of increased mechanical energy. In the following section, the maximum speed of the rocker, 30 rpm, was utilized to simulate the motion of bilgewater under more aggressive mixing conditions.

2.3.5 Oil drop size after dynamic ageing at 30 rpm

Dynamic ageing was increased to 30 rpm, and the tilt angle was increased to increase the energy input into the system. The amount of air within the ageing vial remained constant at 70%. The corresponding oil drop size distributions are shown in **Figure 2.12**. For 10 and 100 ppm of both SLES and Triton X-100, the same trends found in dynamic ageing at 12 rpm apply. That is, there are three peaks at 0.5 μm , 50 μm , and 2 mm, indicating drop breakup and coalescence. However, at 100 ppm SLES, the coalescence of drops 50 μm and 2 mm in diameter was not sufficient to cause an overall increase in $D(4,3)$. At 500 ppm SLES, peaks at 50 μm or 2 mm do not exist, and a transition to smaller oil drop sizes over the 20 days. At 1000 ppm of SLES, a wider distribution between 0.2 – 20 μm appears after 5 days and does not change with time. **Figure 2.13** shows an optical image of 1000 ppm SLES after 20 days of ageing at 30 rpm and includes oil drops sizes well below 50 μm . It is noticeable that stability against coalescence is achieved at SLES concentrations ≥ 100 ppm.

At 500 ppm Triton X-100, there were no 2 mm oil drops present. In turn, the distribution shifts toward 0.2 and 9 μm within 5 days. Between 10 and 20 days, a small peak formed at 50 μm , which demonstrates the coalescence of oil drops; however, there was not enough coalescence to increase the $D(4,3)$ over time. At 1000 ppm, a peak formed between 0.2 – 9 μm within 5 days and did not change much over time. For Triton X-100, stability against coalescence was found at concentrations ≥ 500 ppm. These results indicate that at 30 rpms, the O/W emulsions can form oil drops far below 1 μm and lead to stabilization of oil drops against coalescence.

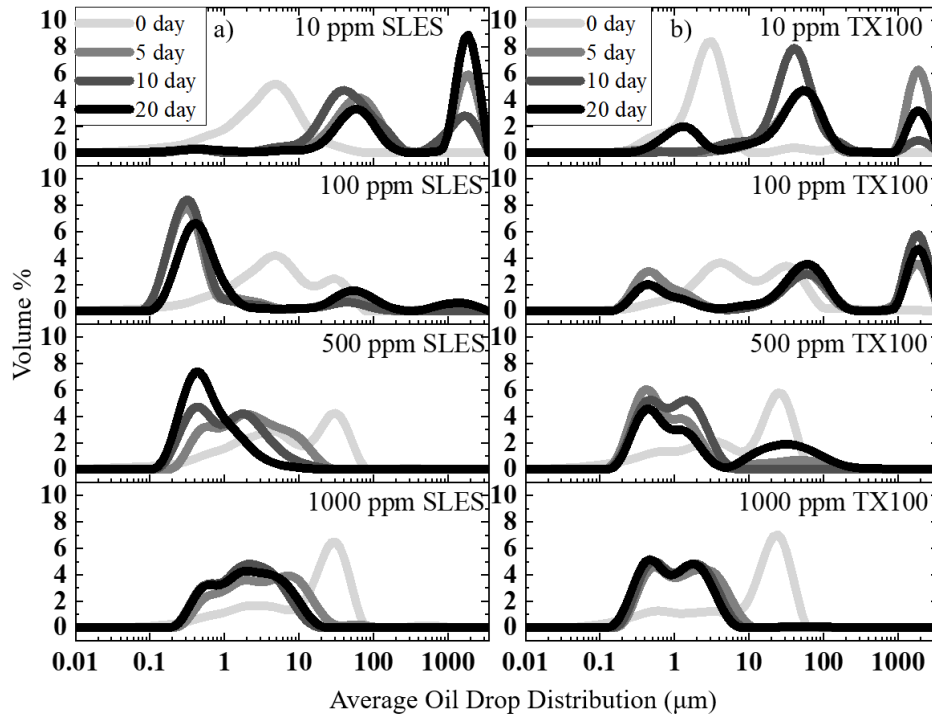


Figure 2.12: The evolution of average oil drop size distribution over 20 days for dynamically aged emulsions with 70% air at 30 rpm with a) SLES and b) Triton X-100 from 100 to 1000 ppm surfactant. The darkening of the distribution curves is proportional to time.

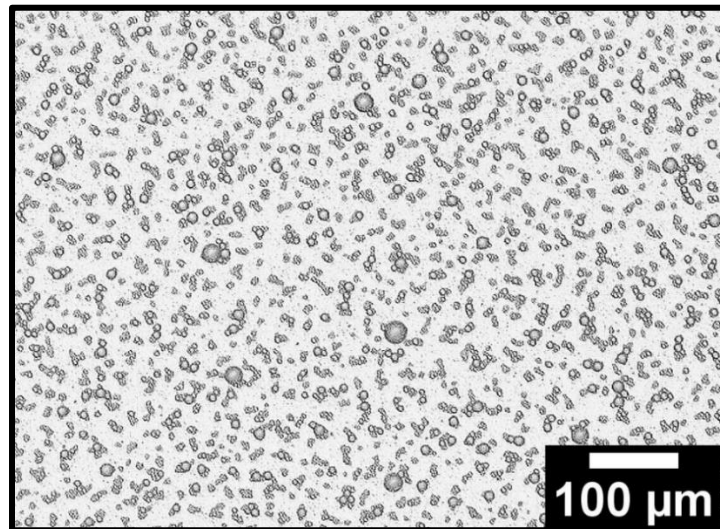


Figure 2.13: Brightfield optical image of an emulsion (0.42M NaCl, 1000ppm SLES, 5000ppm mineral oil) dynamically aged at 30rpm for 20 days and with 70% air within the ageing vial.

Figure 2.14 shows that dynamically ageing emulsions at 30 rpm caused an overall decrease in oil drop size over 10 days for 100 – 1000 ppm SLES and 500 – 1000 ppm Triton X-100, which indicates the formation of small oil drops within the emulsion. For 10 ppm SLES and 10 – 100 ppm Triton X-100, the D(4,3) increased over 20 days, suggesting coalescence. The minimum surfactant concentration required to form stable emulsions for dynamic ageing at 30 rpm is similar to static ageing. However, the oil drop size distributions in **Figure 2.12** revealed that dynamic ageing at 30 rpms produced smaller drops at surfactant concentrations above the stability threshold within 5 days.

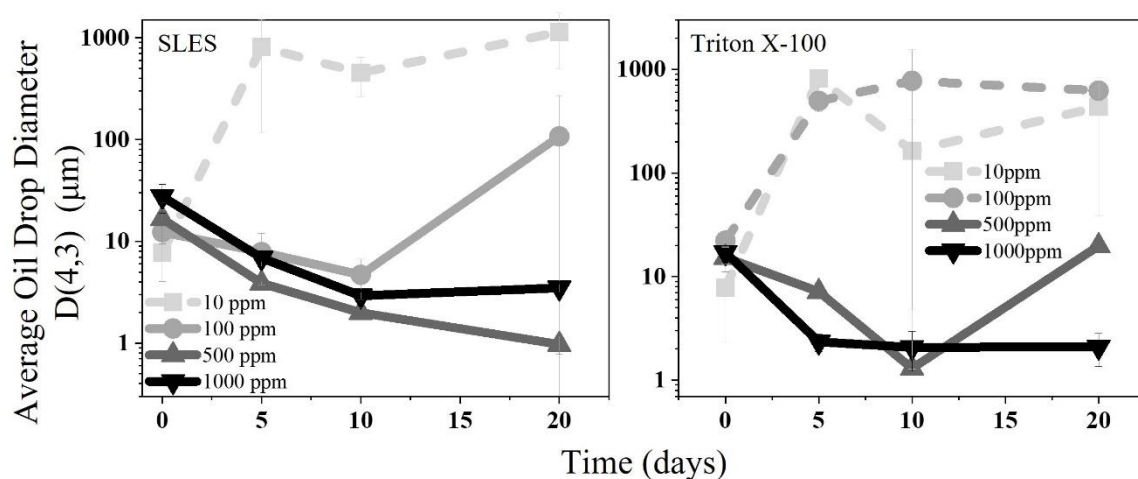


Figure 2.14: Average oil drop diameter, D(4,3) during dynamic ageing with 70% air at 30 rpm and increasing surfactant concentration for SLES (left) and Triton X-100 (right). Dashed lines represent unstable emulsions that result from increased oil drop size over time. The darkening of the lines is proportional to increased surfactant concentration.

The surfactant concentration required to prevent oil drop coalescence was 100 ppm SLES and 500 ppm Triton X-100. The amount of SLES needed to stabilize the emulsions is still less than that of Triton X-100 due to the difference in zeta potential between the surfactant chemistries. Although oil drops stabilized by Triton X-100 have less electrostatic repulsion and can approach each other more closely than SLES-stabilized oil drops, the speed of the 3D rocker was sufficient enough to break larger oil drops and reduce the probability of coalescing oil drops.

The CMCs for SLES and Triton X-100 listed in **Table 2.1** correlate to the stability thresholds during dynamic ageing at 30 rpm and static ageing. For static ageing, emulsions made with a

surfactant concentration above the stability threshold, the oil drop size distribution does not change with time. Dynamic ageing at 30 rpm promoted oil drop breakup, which increased the number of small drops or the interfacial area.⁵⁵ Many small oil drops were stabilized upon increasing surfactant concentration because there was enough surfactant to cover the interfacial area.³⁰ Dynamically aged emulsions (30 rpm) made with a S/O ≥ 0.02 for SLES or ≥ 0.1 for Triton X-100 are still considered stable because the average oil drop size after 20 days was less than 1 μm .

The mechanisms of drop coalescence and drop formation can be explained by the amount of energy the rocker provides for the system. Utilizing the rocker at low speeds or at low energy input increases the drop-drop collision frequency to promote coalescence. Previous work showed how stirred tanks^{35,26} and swirled flasks⁵⁹ were used to observe oil drop breakup and coalescence, which depends on the effectiveness of surfactants. For example, Fingas et al. showed that drop breakup was achieved by swirling O/W emulsions in a flask above 150 rpm.⁵⁹ In contrast, stirred tanks that utilize an impeller to mix emulsions found that at low surfactant concentration, the coalescence rate of oil increased at a stir speed of 460 rpm. However, fine oil drop sizes were achieved at higher concentrations of surfactant.³⁵ Self-emulsification, or emulsification due to little energy input, has also been studied for drug delivery in pharmaceutical industries.⁶⁰ Self-emulsifying systems form emulsions under gentle agitation. Self-emulsifying emulsions with a low concentration of non-ionic surfactants produced an oil drop size distribution with high polydispersity (Polydispersity Index = 7) and contained sub-micron and 100 μm diameter drops.⁶⁰ This behavior is similar to model bilgewater emulsions studied here.

Many other studies have investigated coalescence and drop breakup of emulsions in turbulent shear flows.^{19,32,43} These studies provide examples of other “dynamically” aged emulsions. For example, for the application of oil spill remediation, it was found that over time, large crashing waves dispersed oil slicks to greater depths and produced oil drops 50 μm in diameter in the presence of surfactants.³¹ Other studies^{26,31,34,35,59,60} provide insight into the mechanisms observed, such as drop breakage during dynamic ageing; however, they do not fully model the experimental setup and physical system presented in this paper. Therefore, an estimation of energy density input is required to quantify the behavior of dynamic ageing.

Emulsions made with a surfactant concentration that produced the most changes in oil drop size distributions after 20 days between static ageing and dynamic ageing were chosen to summarize the stability behavior of the emulsions. **Figure 2.15** summarizes the oil drop size distributions that result from emulsions with 100 ppm SLES and 500 ppm Triton X-100 that were statically aged, dynamically aged at low speeds, and dynamically aged at high speeds. The light gray curves represent statically aged emulsions, the dark gray curves show dynamically aged emulsions at 12 rpm, and the black curves represent dynamically aged emulsions at 30 rpm. For both surfactants, drop coalescence and drop formation was observed for dynamic aged emulsions at 12 rpm. It can also be seen that for 100 ppm SLES, dynamic ageing at high energy produced more sub-micron drops than when statically aged or dynamically aged at low energy. These results are similar for 500 ppm Triton X-100. Therefore, the inclusion of motion during ageing is unfavorable for destabilizing emulsions to coalescence due to the formation of sub-micron drops.

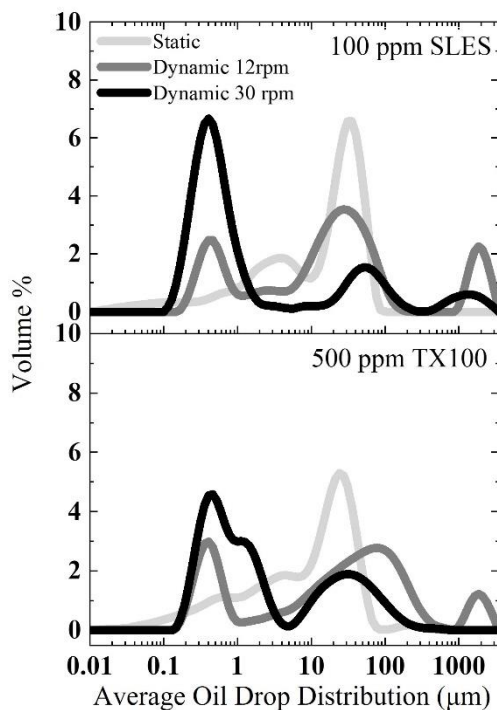


Figure 2.15: Average oil drop size distribution after 20 days for 100 ppm SLES and 500 ppm Triton X-100 aged statically, dynamically at 12 rpm, and dynamically at 30 rpm.

2.4 Conclusions

Overall, dynamically ageing emulsions on a 3D rocker provided a physical representation of ship movement. Shipboard rocking can promote coalescence or emulsification depending on rocking speed, surfactant concentration, and surfactant type. The results presented in this paper verify the expectation that there is a minimum amount of surfactant required to make a thermodynamically stable emulsion.

- For statically aged emulsions, the S/O ratio required for stable emulsions was 0.02 for SLES and 0.1 for Triton X-100. Specifically, at a constant oil volume fraction, the concentration of SLES to prevent coalescence was three times the CMC.
- For dynamically aged emulsions, the S/O required for stable emulsions was 0.2 for either surfactant. Thus, dynamic ageing provided more energy to the system and increased the amount of surfactant needed to resist coalescence for 20 days. During dynamic ageing, an interplay exists between drop breakup and coalescence. However, if the S/O ratio was greater than 0.2 for either surfactant, coalescence was not observed, and drop breakup dominated the system.
- SLES was more effective in stabilizing the emulsions than Triton X-100, but if added in excess, Triton X-100 hindered coalescence as compared to SLES.
- Ship motion can promote coalescence at low surfactant concentrations.

A solution to prevent emulsion formation during ship rocking includes the possible redesign of the bilge tank by investigating the behavior of O/W emulsions when the amount of air within the emulsification chamber is reduced during dynamic ageing. At 70% air inside the ageing vial, sloshing is responsible for drop formation and coalescence. Therefore, reducing the amount of air within the emulsification chamber will limit the sloshing and inhibit further emulsion formation and possible coalescence. A more detailed study of this hypothesis will be investigated in Chapter 3.

3. IMPACT OF LOW ENERGY MIXING ON THE STABILITY OF OIL-WATER EMULSIONS WITH ANIONIC AND NON-IONIC SURFACTANTS IN HIGH SALINITY WATER.

3.1 Introduction

As discussed in Chapter 2, surfactants enhance the stability of bilgewater emulsions formed due to cleaning and the movement of discharged fluid through pipes before entering the bilge tank. Once collected, bilgewater emulsions are further emulsified due to the sloshing imposed by the ship's motion at sea.

In Chapter 2, dynamic ageing was established by subjecting the emulsions to motion during storage via a 3-dimensional rocker at a fixed speed. The effect of ship motion via dynamic ageing was compared to static ageing by measuring the evolution of oil drop size distributions. The original experiments emulsified 15 mL of a solution with anionic or non-ionic surfactants, sodium chloride, and mineral oil in a 50 mL centrifuge tube to prevent overflow during emulsification in the high shear mixer. The centrifuge tube, or ageing vial, contained roughly 70% of air when placed on the 3-dimensional rocker. Onboard, it can be assumed that there is a certain amount of free volume present in the bilge tank at any given time. Once the emulsions were placed on the rocker, the liquids experienced splashing due to the volume of air present, which encouraged emulsification or coalescence, depending on surfactant concentration. The work presented in this chapter hypothesizes that it is possible to minimize further emulsification by eliminating sloshing motion in the collection tank.

This chapter reports the results of experiments that use the same model O/W emulsions in Chapter 2 to compare the evolution of oil drop size distributions under two conditions: dynamic ageing with mostly air inside the vial (Chapter 2) and dynamic ageing with no air inside the vial. The evolution of oil drop size distributions was measured similarly as in Chapter 2 for proper comparison. In Chapter 2, the stability of statically and dynamically aged emulsions is dependent on the surfactant concentration. Therefore, we hypothesize that if the extra emulsification due to motion is reduced or eliminated, dynamically aged emulsions will exhibit similar stability to statically aged emulsions with respect to surfactant concentration.

3.2 Materials and Methods

3.2.1 Emulsion preparation

Model bilge water emulsions were prepared exactly as in Chapter 2. The surfactants used to prepare the O/W emulsions were anionic sodium lauryl ether sulfate (SLES) (STEOL US-170UB, Stepan Co., molecular weight = 332.4 g/mol) and non-ionic Triton X-100 (Sigma- Aldrich, Laboratory-grade, molecular weight = 625 g/mol) used at concentrations of 10, 100, 500, and 1000 ppm. Heavy mineral oil (Sigma- Aldrich) was used as the dispersed phase at 5000 ppm. The aqueous phase of the emulsion consisted of 0.42 M sodium chloride (NaCl) to represent the concentration of seawater. The total volume of the emulsions was 15 mL, and the liquids were emulsified in a 50 mL centrifuge tube. A high shear mixer (VWR VDI 25) was used to emulsify each sample at 24,000 rpm for 1 minute to form oil drops around 20 μm in diameter.

Immediately after emulsification, the liquids were dispensed into 50 mL syringes of the same diameter as the centrifuge tube (25 mm). Two conditions were tested in which air was expelled from the syringe so that there was either 50% of air inside the tube or 0% air inside the tube. In the latter condition, the emulsion occupied 100% of the volume. Surfactant foam and bubbles produced from emulsification destabilized within 3 hours, to which all the air was successfully expelled from the syringe. Throughout this document, these samples will be referred to as emulsions with 50% air and 0% air. **Figure 3.1** shows photographs of the emulsification chamber for 70%, 50% and 0% air emulsions.

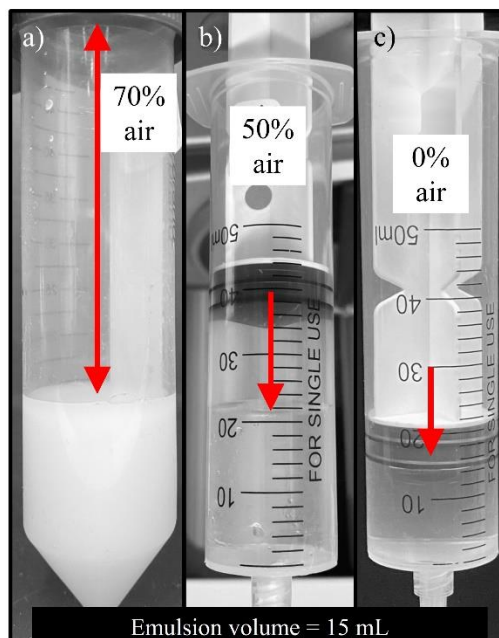


Figure 3.1: Photographs of a 15 mL emulsion inside a) a 50 mL centrifuge tube with 70% air, b) a syringe with 50% air and c) a syringe with all air removed (0% air).

3.2.2 Emulsion ageing conditions and characterization

Ship rocking due to sea waves was replicated via dynamic ageing. A three-dimensional rocker (Benchmark BenchRocker 3D Nutating Shaker) was used and set at 30 rpm and a tilt angle of 24 degrees. The air-capped emulsions were placed on the 3D rocker at 30 rpm for 5, 10, and 20 days. This set of experiments will be compared to emulsions with 70% air that were statically and dynamically aged in Chapter 2.

The oil drop distribution was measured via laser diffraction (Malvern Mastersizer 3000) after 5, 10, and 20 days for the air-capped emulsions. Optical microscopy was used with an Olympus BX41 Microscope and AM Scope software to visualize the distribution of oil drops for some emulsions.

3.2.3 Energy density for dynamic ageing

An initial estimation for the energy density input for dynamic ageing was derived in Chapter 2. This estimation was based on the balance between the potential and kinetic energy of a falling

object. This approach found that for 20 days of ageing, 8.83 J/mL was provided by the rocker for emulsions with 70% air (Chapter 2). According to this equation, it is predicted that emulsions with 0% air will experience 0 J/mL of energy during dynamic ageing, to which the oil drop distribution does not change over time. However, this prediction is questionable since oil drops can move throughout the aqueous phase due to density differences between mineral oil and saltwater.

3.3 Results and Discussion

3.3.1 Effect of dynamic ageing with 50% and 0% air inside the ageing vial

After initial emulsification in the high shear mixer, emulsions were placed in a syringe 50% of the air was expelled to reduce the amount of splashing during dynamic ageing. **Figure 3.2a** and **Figure 3.2b** shows the oil drop size distributions over 20 days for emulsions with 10 – 1000 ppm SLES and Triton X-100, respectively, that have been dynamically aged at 30 rpm with 50% air inside the ageing vial. For emulsions with 10 ppm SLES, the distribution indicates that after 20 days, the emulsions were unstable due to coalescence. For 100 – 500 ppm SLES, the curves at 0 days consist of two peaks at 20 μm and 5 μm . After 5 days, the distributions shift to a single peak centered at 0.5 μm and remains stable throughout the 20 days. This indicates that once the 0.5 μm oil drops are formed, they are stabilized by SLES.

For Triton X-100 emulsions, the behavior of the evolution of the oil drop distribution for 10 ppm is similar to 10 ppm SLES in that the oil drops coalesce over time due to insufficient surfactant concentration. For 100 ppm Triton X-100, the distribution at 0 days consists of two peaks at 20 and 5 μm . After 5 days, the distribution shifts to form three peaks at 0.5 μm , 200 μm and 2mm. After 10 days, the height of the peak at 0.5 μm drops increases as the peaks at 200 μm and 2mm no longer exist. However, after 20 days, the peak at 200 μm reappears and the height of the peak at 0.5 μm drops decreases. For 500 – 1000 ppm Triton X-100, the bimodal peaks at 0 days shifts to a singular peak at 0.5 μm after 10 days. After 20 days, the height of the peak at 0.5 μm decreases and a peak at 200 μm appears.

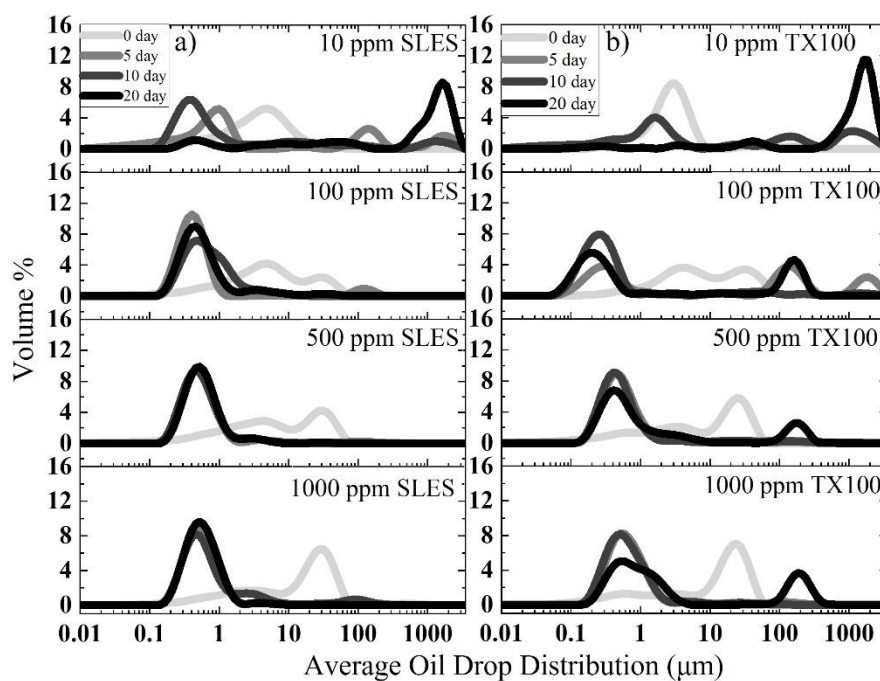


Figure 3.2: The evolution of average oil drop distribution over 20 days for dynamically aged emulsions with 50% air and concentrations from 10 – 1000 ppm of SLES. The darkening of the distribution curves is proportional to time.

Because there was less air in the ageing vial for emulsions with 50% air than emulsions with 70% air, it was expected that the generation of sub-micron oil drops would occur more slowly over time. For example, **Figure 2.12a** shows that for 500 ppm SLES with 70% air, the distribution gradually shifts from 20 μm at 0 days to 0.5 μm at 20 days. Therefore, it was expected that for emulsions with 50% air, there would be less sloshing that occurred, and the opportunity for oil drops to break up into sub-micron sizes would be reduced. However, **Figure 3.2a** indicates that for 500 ppm SLES, sub-micron drops were generated after 5 days. Overall, the oil drop sizes that were present after 20 days for emulsions with 100 – 1000 ppm SLES and 50% air are similar to the sizes present after 20 days for the same emulsions with 70% air. For Triton X-100 emulsions with 50% air, the appearance of a peak at 200 μm after 20 days indicates that when air is removed from the ageing vial, larger drops are formed due to coalescence. This may be explained by the fact that Triton X-100 is ineffective in stabilizing the sub-micron drops over time as SLES.

Overall, it was expected that sloshing would be reduced upon reducing the amount of air within the ageing vial, which would reduce the velocity at which oil drops collide. Therefore, it would take longer for oil drops to break up into sub-micron sizes. However, this was not the case, as sub-micron drops were formed after 5 days and remained throughout the duration of ageing.

In a second condition, all the air was expelled to eliminate any splashing during dynamic ageing. As stated in Chapter 2, mineral oil drops larger than $2.8\ \mu\text{m}$ are desired as they are large enough to cream to the surface and remove. All emulsions aged with 0% air inside the ageing vial experienced creaming. **Figure 3.3** shows a creamed layer in an emulsion made with 100 ppm SLES.

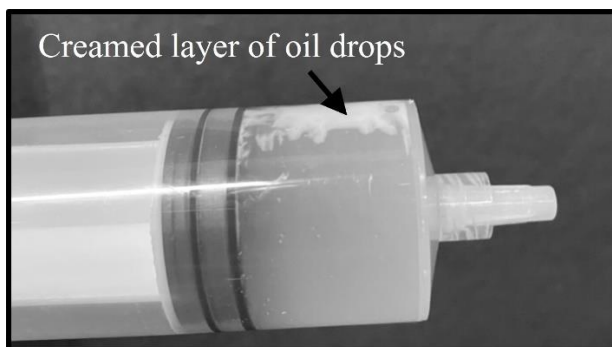


Figure 3.3: Photograph of an emulsion dynamically aged for 5 days with 100 ppm SLES, 0.42 M sodium chloride, 5000 ppm mineral oil, and 0% air.

Figure 3.4a and **Figure 3.4b** show the oil drop distributions over 20 days for SLES and Triton X-100, respectively. For 10 ppm Triton X-100, the average size of the oil drops was too large to be measured via laser diffraction after 5 days. This was the result of coalescence during ageing. For emulsions with 10 ppm SLES, the distribution varied over time and resulted in three separate peaks (at $0.5\ \mu\text{m}$, $10.5\ \mu\text{m}$, and $2\ \text{mm}$) after 20 days. The accuracy of the curves for 10 ppm SLES is unreliable for similar reasons to emulsions with 10 ppm Triton X-100. Coalescence was observed for 10 ppm SLES and is shown in **Figure 3.5**. For 100 ppm SLES, the curve at 0 days consisted of a major peak at $9\ \mu\text{m}$ and a secondary peak at $12\ \mu\text{m}$. Within 5 days, the peak at $12\ \mu\text{m}$ disappeared, and the peak at $9\ \mu\text{m}$ remained. After 10 days, the peak shifted towards $2\ \mu\text{m}$, and two new peaks were measured at $0.5\ \mu\text{m}$ and $100\ \mu\text{m}$. After 20 days, the height of the peak at 0.5

μm and $100\ \mu\text{m}$ decreased while the height of the peak at $2\ \mu\text{m}$ increased. A small peak at $200\ \mu\text{m}$ also existed after 20 days. At 500 ppm SLES, the oil drop distribution at 0 days and 5 days was nearly identical. After 10 and 20 days of ageing, the distribution shifted to a peak ranging from $0.2 - 10\ \mu\text{m}$ and a small peak at $200\ \mu\text{m}$. At 1000 ppm SLES, there is an exchange in the volume % of oil drops that were $20\ \mu\text{m}$ at 0 days to oil drops between $0.2 - 10\ \mu\text{m}$ at 20 days. However, a small peak at $200\ \mu\text{m}$ was measured after 20 days. The change in the oil drop size over time shows that although there was no sloshing inside the syringe, coalescence and drop generation occurred. **Figure 3.6** shows optical images of emulsions at each concentration of SLES after 20 days to support the measured oil drop distributions in **Figure 3.4a**.

The evolution of oil drop distributions over 20 days for emulsions with 0 % air and Triton X-100 is shown in **Figure 3.4b**. Again, the evolution of oil drop size distribution was not measured for 10 ppm Triton X-100. For 100 ppm Triton X-100, the distribution at 0 days consists of one peak at $40\ \mu\text{m}$ and one at $4\ \mu\text{m}$. After 5 days, the distribution shifted to consist of a major peak centered at $8\ \mu\text{m}$ and a minor peak around $0.6\ \mu\text{m}$. After 10 days, the peak at $0.6\ \mu\text{m}$ remained, and the major peak at $8\ \mu\text{m}$ now shifted to $6\ \mu\text{m}$, indicating drop breakup. After 20 days, the peak at $6\ \mu\text{m}$ shifted in the opposite direction toward $25\ \mu\text{m}$, and a new peak at $2\ \text{mm}$ was measured. The peak at $0.6\ \mu\text{m}$ remained. For concentrations ≥ 500 ppm Triton X-100, the distributions evolved similarly to that of 1000 ppm SLES. For example, there was an exchange in the volume % of $20\ \mu\text{m}$ oil drops at 0 days to $0.3 - 8\ \mu\text{m}$ oil drops at 20 days. A small peak at $200\ \mu\text{m}$ existed after 20 days for 500 ppm and 1000 ppm Triton X-100.

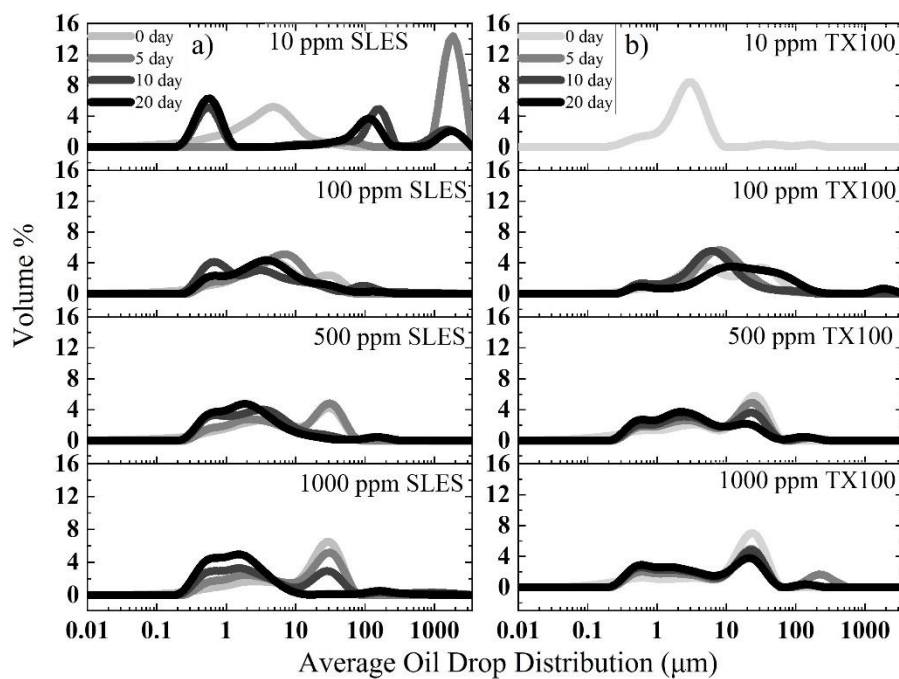


Figure 3.4: The evolution of average oil drop distribution over 20 days for dynamically aged emulsions with 0% air and concentrations from 10 – 1000 ppm of SLES. The darkening of the distribution curves is proportional to time.

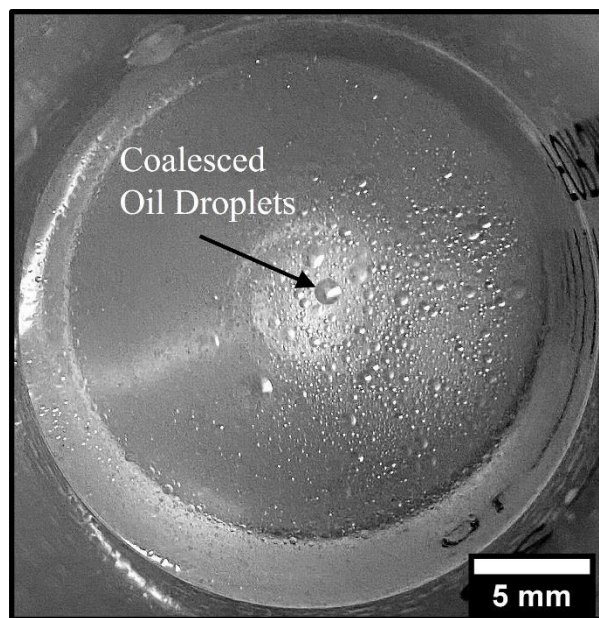


Figure 3.5: Top view photograph of coalesced mineral oil drops in an emulsion with 10 ppm SLES, 0.42 M sodium chloride, and 5000 ppm mineral oil after 20 days of ageing with 0% air inside the syringe.

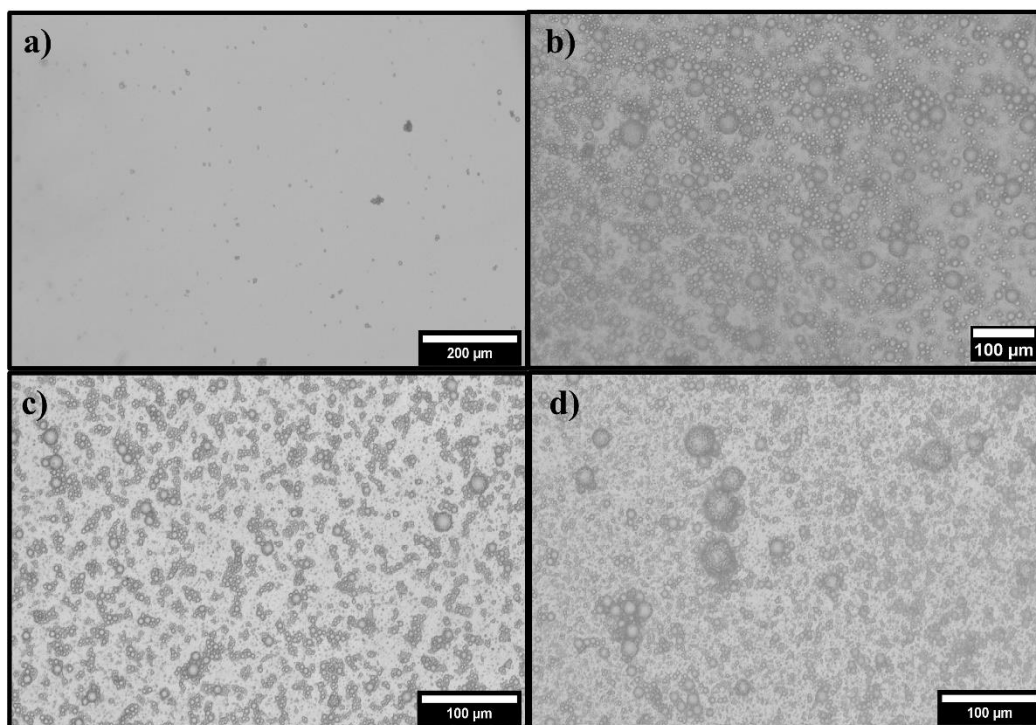


Figure 3.6: Brightfield optical images of a) 10 ppm b) 100 ppm c) 500 ppm and d) 1000 ppm SLES after 20 days of dynamic ageing with 0% air inside the syringe.

Earlier, it was predicted that dynamic ageing of emulsions with 0 % air imparts 0 J/mL. If this were true, the evolution of oil drop size distributions would look identical to the distributions statically aged emulsions in Chapter 2, section 3.3. Instead, the oil drop size distribution shifted toward smaller sizes for emulsions with ≥ 500 ppm SLES or Triton X-100.

One explanation for the breakup of oil drops in air-capped emulsions during dynamic ageing arises from the difference in density between oil and water. As established earlier, removing the free space within the emulsification chamber successfully eliminated any splashing during dynamic ageing. However, the density of mineral oil (0.86 g/mL) is less than that of saltwater with 0.42 M NaCl (1.023 g/mL). Therefore, mineral oil drops shear against the aqueous phase during dynamic ageing even when there is no air inside the ageing vial. The speed at which the oil drops move depends on their size. Over time, the oil drops collide with one another and either break up into smaller oil drops or coalesce, which can be seen by the shift in oil drop size distribution toward

smaller and larger sizes, shown in **Figure 3.4**. The extent to which oil drop breakup occurs depends on surfactant concentration. At a surfactant concentration ≥ 100 ppm SLES or ≥ 500 ppm Triton X-100, the interfacial tension between mineral oil and the surfactant and salt solutions decreases to 2.7 mN/m and 3.5 mN/m, respectively (Chapter 2). Here, the energy required to break up oil drops is less than that for emulsions with < 100 ppm SLES or < 500 ppm Triton X-100. Therefore, at concentrations ≥ 100 ppm SLES or ≥ 500 ppm Triton X-100, drops are broken into a given size, to which there is enough surfactant to cover the interfacial area.

For all dynamically aged air-capped emulsions, creaming was experienced, and the average oil drop size was above 2.8 μm in diameter, regardless of surfactant concentration. However, sub-micron drops were formed in emulsions with a S/O greater than 0.01 for either surfactant during dynamic ageing. A greater number of sub-micron oil drops were formed for dynamically aged emulsions with 70 % air inside the ageing vial (Chapter 2). No matter the extent, the generation of sub-micron oil drops is unfavorable for bilgewater emulsions. Ship rocking is unavoidable and causes bilgewater to further emulsify due to the sloshing of the liquids. Mitigating the sloshing by removing air from the ageing vial does not entirely prevent the formation of sub-micron oil drops due to the difference in density between oil and water.

3.3.2 Effect of dynamic ageing on the dispersion of oil into surfactant and salt solutions

Prior to this section, the liquids were pre-mixed to represent bilgewater that has been pumped through pipes and tanks before entering the bilge tank. In this section, emulsions were dynamically aged *without* being pre-emulsified in the high-shear mixer to represent a situation in which a volume of oil is dispensed on the surface of bilgewater and is subjected to ship rocking over time. **Figure 3.7** shows a bulk volume of oil that was placed on the surface of a solution with SLES and salt. It is important to note that the mineral oil volume fraction of the emulsions was only 0.0058 (5000 ppm). These preliminary results will provide some evidence for the effect of ultra-low energy input via dynamic ageing on the emulsification of model bilgewater liquids. The energy provided during dynamic ageing is significantly less than the energy added during initial emulsification via high shear mixing. For example, after 10 days of dynamic ageing, it was estimated that 4.4 J/mL of energy is added to an emulsion with 70% air inside the ageing vial. This is compared to 162 J/mL added during high shear mixing. The following section provides

preliminary results from dynamic ageing without pre-emulsifying the liquids under the two previously established scenarios: dynamic ageing with 0% and 70% air inside the ageing vial. Scenario 1 consists of emulsions with 10 – 1000 ppm SLES were subjected to dynamic ageing with 0% air. Scenario 2 consists of emulsions with 10 – 1000 ppm SLES or Triton X-100 that were subjected to dynamic ageing with 70% air. The oil drop sizes were analyzed for each scenario after 10 days.

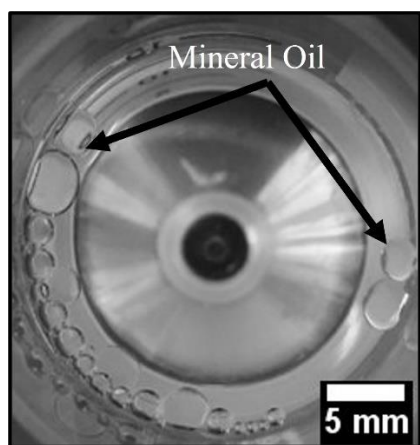


Figure 3.7: Photograph of the top view of a SLES and salt solution with 5000 ppm mineral oil added to the surface (0 days aged).

Scenario 1: Dynamically ageing non-pre-mixed emulsions with 0% air

In the first scenario, 5000 ppm mineral oil, 0.42 M NaCl, and various surfactant concentrations were placed into a syringe to which all the air was expelled before dynamic ageing at 30 rpm for 10 days. Again, the oil was not pre-emulsified. All emulsions were transparent after 10 days of ageing and the oil drop size was too large to measure via laser diffraction. **Figure 3.8a** and **Figure 3.8b** show photographs of the surface of emulsions with 10 ppm and 1000 ppm SLES that were aged for 10 days with 0% air.

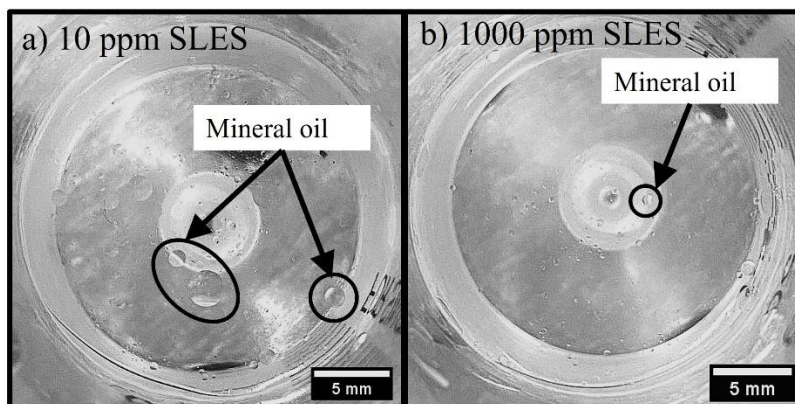


Figure 3.8: Photographs of the top view of emulsions with a) 10 ppm SLES and b) 1000 ppm SLES, 0.42 M sodium chloride, and 5000 ppm mineral oil that were not pre-emulsified and dynamically aged with 0% air for 10 days.

The average oil drop size was larger for 10 ppm SLES than for 1000 ppm SLES. This trend is expected, as there is enough surfactant to cover the oil-water interface for 1000 ppm SLES. Nevertheless, dynamically ageing the non-pre-mixed and air-capped emulsions showed signs of reduction in initial oil drop size over time due to the difference in density between mineral oil and salt water. Since all emulsions that were dynamically aged with 0% air were transparent after 10 days, it can be assumed that a great number of sub-micron drops were non-existent; however, the oil drop size within the subnatant was not measured. Regardless of surfactant concentration, the oil drops formed were large enough to cream to the surface. The implications of these results indicate that the formation of sub-micron droplets can be prevented if the amount of free space in the bilge tank is reduced and if the bilgewater initially contained only millimeter-sized oil drops. However, the latter condition is difficult to achieve as micron-sized oil drops are likely present in bilge water after being pumped through a series of pipes and tanks prior to filtration.

These results indicate that the energy produced by the oil shear against the tube walls is not enough to generate sub-micron drops. Consequently, if sloshing during dynamic ageing is not significant, there is not enough energy to promote drop breakup. Therefore, a more complex process must be driving the changes in drop size distributions for emulsions that were pre-mixed and dynamically aged with 0% air inside the ageing vial.

Scenario 2: Dynamically ageing non-pre-mixed emulsions with 70% air

Figure 3.9 shows the oil drop size distributions after 10 days of dynamic ageing with 70% air for SLES and Triton X-100. These samples were not pre emulsified and 5000 ppm mineral oil was dispensed on top of the surfactant solution prior to ageing. Therefore, the oil drop size distribution at zero days for both surfactants is not included in **Figure 3.9**, as the oil drop sizes were too large to measure via laser diffraction. Recall that **Figure 3.7** shows an image that represents the oil drop sizes at zero days for all emulsions. For either surfactant, there is a reduction in oil drop size from 0 to 10 days of dynamic ageing. For 10 ppm SLES, part of the bulk oil was emulsified into droplets around 0.5 μm , 2 μm , 100 μm , and 2 mm as indicated by the four peaks. For 100 ppm SLES, the bulk oil was emulsified into droplets around 0.5 μm and 10 μm in diameter after 10 days. At 500 ppm SLES, one major peak existed at 100 μm and two minor peaks existed at 20 μm and 2 mm. Lastly for 1000 ppm SLES, a unimodal distribution was measured and centered at about 100 μm . **Figure 3.10** verifies the oil drop size distributions for 10 ppm and 1000 ppm SLES and **Figure 3.11** shows images of the evolution of oil drop size for 1000 ppm SLES over 2 days.

Similar behavior for Triton X-100 is presented in **Figure 3.9b**. At 10 ppm Triton X-100, one major peak was measured at 50 μm . As the concentration of Triton X-100 increased to 100 ppm, a peak at 0.5 μm was measured. For both 500 ppm and 1000 ppm Triton X-100, two peaks existed at 40 μm and 2 mm.

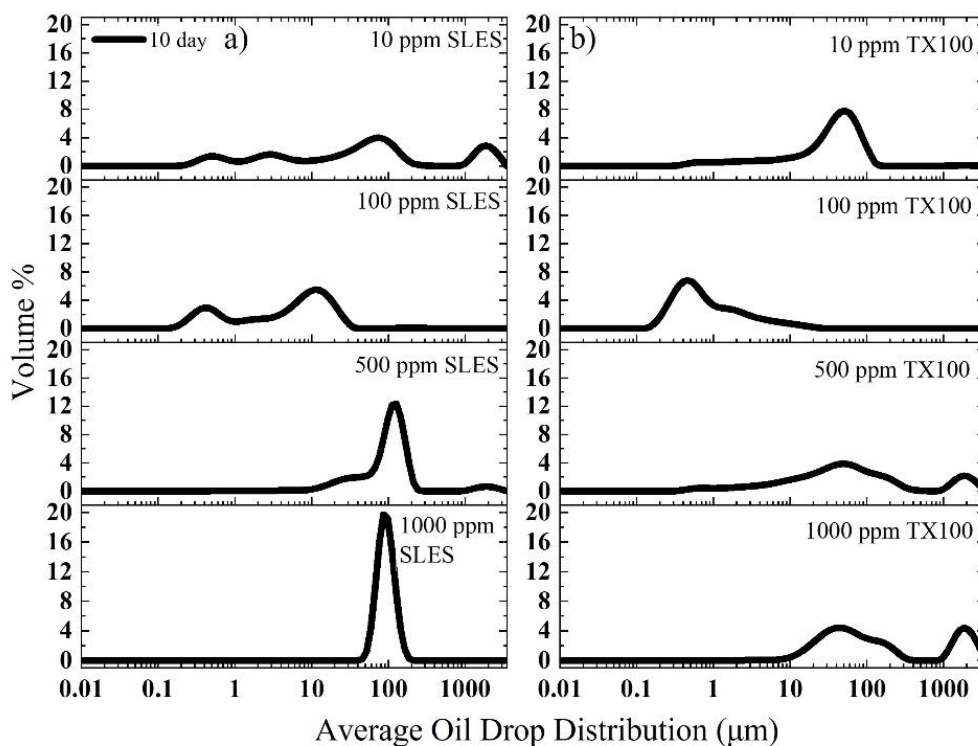


Figure 3.9: The average oil drop distribution for 10 – 1000 ppm of a) SLES and b) Triton X-100 after 10 days of dynamic ageing with 70% air. Mineral oil (5000 ppm) was dispensed, and the liquids were not pre-emulsified prior to ageing.

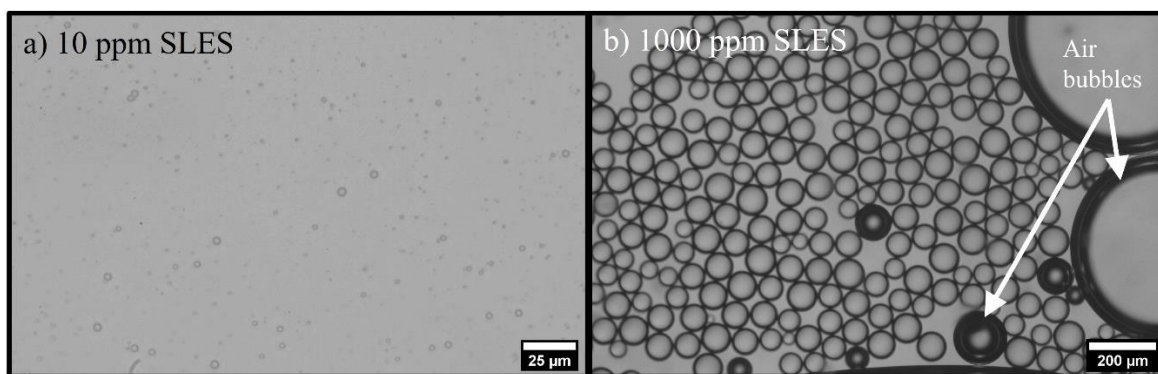


Figure 3.10: Brightfield optical images of a) 10 ppm and b) 1000 ppm SLES, 0.42 M sodium chloride, and 5000 ppm mineral oil after 10 days of dynamic ageing with 70% air and no pre-mixing.

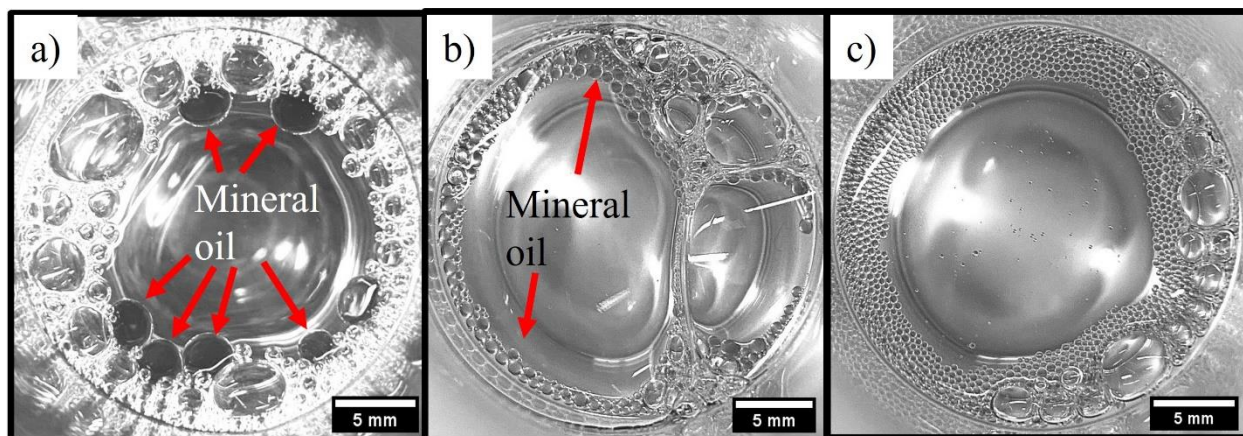


Figure 3.11: Top view photographs of an emulsion with 1000 ppm SLES, 0.42 M sodium chloride, 5000 ppm Mineral oil after a) 0 days, b) 5 hours, and c) 2 days of dynamic ageing with 70% air and no pre-mixing.

After 10 days of dynamic ageing with 70% air, both 10 ppm and 100 ppm SLES emulsions were optically opaque, indicating that sub-micron drops exist. This is verified through the oil drop size distributions for 10 ppm and 100 ppm SLES shown in **Figure 3.9**. **Figure 3.12** shows an optical image of an emulsion with 100 ppm SLES that appears cloudy, however there was bulk oil that remained at the surface of the emulsion was not emulsified during dynamic ageing. Since the emulsions were not pre-mixed, the oil initially existed as one large drop at the surface of the surfactant solution. As dynamic ageing begun, the oil drop was stretched and broken into smaller drops. After 10 days, an opaque emulsion was formed after stretching and pinching of the oil which generated micron-sized oil drops that were stabilized by surfactant. However, a large oil drop existed on the surface of the emulsions after ageing.

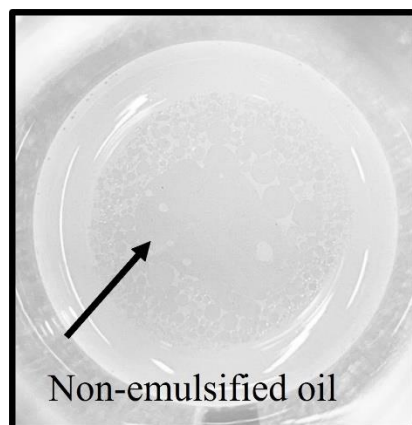


Figure 3.12: Photograph of the top view of an emulsion with 100 ppm SLES, 0.42 M sodium chloride, and 5000 ppm mineral oil after 10 days of dynamic ageing with 70% air and no pre-mixing.

To understand these results, we must first consider the effect of wave motion on oil droplet formation. Several published experiments have attempted to understand the formation of oil droplets due to crashing waves.^{31, 44, 63–66} The application for this investigation arises from oil spill remediation. When a large volume of oil is spilled out into the ocean, surfactants are added to the surface of the ocean where the oil was spilled to disperse the oil throughout the ocean. The energy provided by waves breakup the oil slick into droplets whose size depends on the energy of the wave, the type and concentration of surfactant used^{31, 44}, and the interfacial tension between the oil and water.⁶³ Using a wave-tank apparatus, the work by Li et. Al established that the energy provided by a crashing wave was large enough to form sub-micron oil droplets at a S/O of 0.04.^{31, 44} The sub-micron droplets existed at greater depths than that of the larger drops. The sub-micron droplets are well dispersed by ocean currents and dominated by Brownian motion so that they may never reach the surface. The larger drops were dominated by a buoyancy force that caused them to coalesce and cream to the surface where they are influenced by surface and wind currents.⁶⁵ This causes the bulk oil to stretch in a non-uniform manner caused by a reduction in interfacial tension between oil and water in the presence of surfactants.⁶³ This behavior was seen in for 10 and 100 ppm SLES.

As the concentration of SLES or Triton X-100 was increased to 500 ppm and 1000 ppm, the emulsified droplets were larger than that of 10 ppm or 100 ppm SLES or Triton X-100. It is well known that the oil droplet size decreases with surfactant concentration, however, this is not the

case for these emulsions. A justification to these results is explained by depletion flocculation from the formation of surfactant micelles. It has been estimated that the critical micelle concentration (CMC), or the concentration at which micelles form was around 30 ppm SLES and 300 ppm Triton X-100 for this system (**Table 2.1**). Therefore, emulsions with 500 ppm and 1000 ppm SLES or Triton X-100 will form micelles within the solution. The amount of surfactant that does not contribute to the formation of a micelle is available to adsorb to the oil-water interface. Consequently, the concentration of surfactant at the oil-water interface is less than that of the amount of surfactant initially added to the emulsion due to the formation of micelles. Therefore, the size of the oil drops is limited by the energy provided by dynamic ageing (4.4 J/mL after 10 days).

A limitation of the experiments in Scenario 1 and Scenario 2 Scenario 2: Dynamically ageing non-pre-mixed emulsions with 70% air exists due to the fact that it is unlikely for bilgewater not to be emulsified after collection and treatment. However, the results from Scenario 2 were intriguing in that a narrow drop size distribution with an average size of 100 μm was produced after 10 days for an emulsion with an S/O of 0.2 SLES (1000 ppm SLES, 5000 ppm mineral oil). Therefore, this technique could be advantageous to industries that aim to fabricate large quantities of monodisperse particles. In the following section, emulsions with various surfactant-to-oil ratios were dynamically aged to produce a narrow drop size distribution.

3.3.3 Surfactant-to-oil ratios that produce narrow drop size distributions

In Scenario 2, a narrow drop distribution was formed after 10 days for a dynamically aged emulsion with 1000 ppm SLES, 0.42 M NaCl, 5000 ppm mineral oil, and 70% air within the ageing vial. This section presents preliminary data that aims to investigate different emulsion compositions that produce a unimodal drop size distribution under the same ageing conditions and viscosity's impact on dynamically aged emulsions. The emulsions in this section were not pre-emulsified prior to ageing. **Table 3.1** lists the emulsion compositions and corresponding S/O's used for the following experiments, and **Table 3.2** lists the density and viscosity of heavy and light mineral oil.

Table 3.1: Emulsion compositions used to investigate unimodal drop distributions after dynamic ageing.

Emulsion	SLES concentration (ppm)	Mineral Oil Type	Oil Concentration (ppm)	S/O	NaCl Concentration (M)
1	1000	Heavy	5000	0.2	0.42
2	1000	Heavy	15,000	0.07	0.42
3	1000	Heavy	10,000	0.1	0.42
4	3000	Heavy	15,000	0.2	0.42
5	1000	Light	15,000	0.07	0.42
6	1000	Light	10,000	0.1	0.42
7	3000	Light	15,000	0.2	0.42

Table 3.2: Light and heavy mineral oil density and viscosity at 40°C

Mineral Oil Type (Sigma Aldrich)	Density (g/mL)	Viscosity at 40°C (10^{-3} Pa*s)
Heavy	0.862	57.8
Light	0.846	13.2

Recall that **Figure 3.10b** shows an optical image of Emulsion 1. **Figure 3.13** shows optical images of emulsions 2 – 4 that were dynamically aged for 10 days with heavy mineral oil. The oil drops appear to be less uniform in diameter in **Figure 3.13a** and **Figure 3.13b** than in **Figure 3.13c**. **Figure 3.14** shows optical images of emulsions 5 – 7 that were dynamically aged for 10 days with light mineral oil. Here, the uniformity of drop diameter increases with S/O similar to the emulsions in **Figure 3.13**; however, the drops in **Figure 3.13c** appear more uniform in diameter than **Figure 3.14c**. Therefore, at a constant S/O, the viscosity of the oil impacts how uniform the drops are in diameter. For example, since light mineral oil has a lower viscosity than heavy mineral oil, it is more susceptible to perturbations during dynamic ageing. To confirm that hypothesis, the interfacial tension between light mineral oil and SLES must be measured and analyzed.

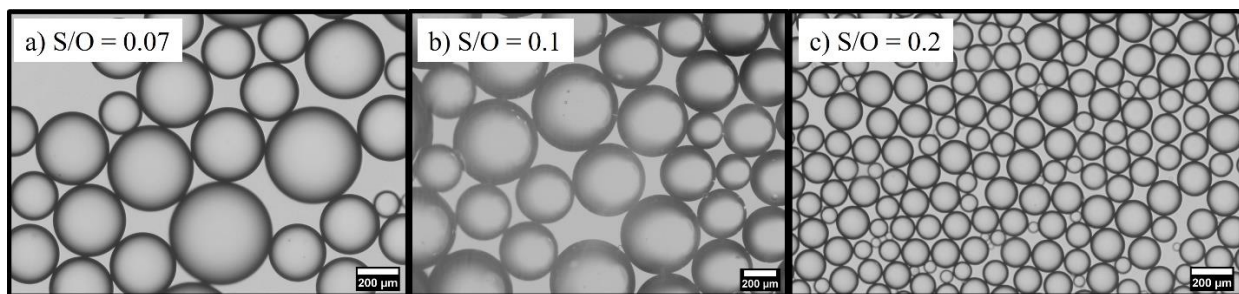


Figure 3.13: Optical Images of emulsions a) 2, b) 3, and c) 4 that were dynamically aged for 10 days at 30 rpm with 70% air within the ageing vial. The emulsions were made with heavy mineral oil and were not pre-mixed prior to ageing.

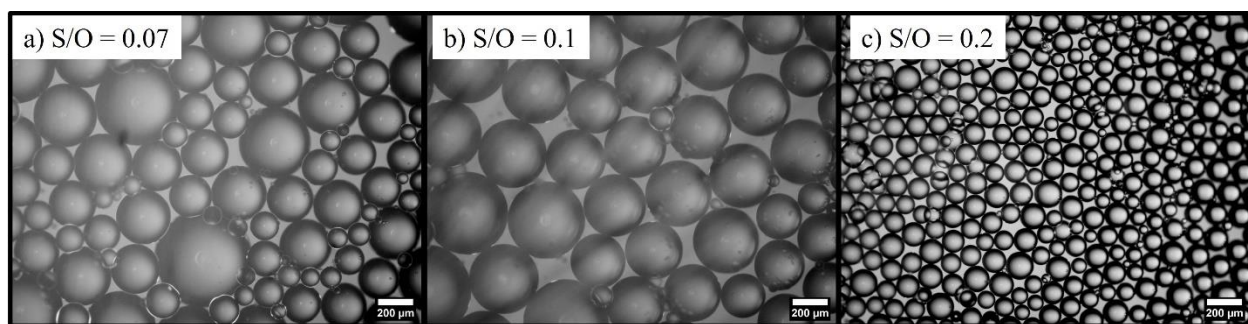


Figure 3.14: Optical Images of emulsions a) 5, b) 6, and c) 7 dynamically aged for 10 days at 30 rpm with 70% air within the ageing vial. The emulsions were made with light mineral oil and were not pre-mixed prior to ageing.

While the oil drops in **Figure 3.13c** are not perfectly monodisperse, they appear to have a narrow distribution in size, which may be favorable for foods, cosmetics, and other industries that need to produce large quantities of drops of similar sizes. This technique of dynamic ageing without prior mixing provides a way to fabricate similar-sized oil drops that is easy and cost-effective.

3.4 Conclusions

Overall, the average oil drop sizes produced during dynamic ageing depend on the surfactant concentration, surfactant type, and free space within the ageing vial.

For pre-mixed emulsions,

- When there was 50% air inside the ageing vial, sub-micron drops were formed within 5 days of dynamic ageing for emulsions with a $S/O \geq 0.02$ for SLES and Triton X-100.

- For the air-capped emulsions, the average oil drop size for all surfactant concentrations was above 1 μm .
- All air-capped emulsions experienced creaming during dynamic ageing. Still, sub-micron oil drops were formed at a $S/O \geq 0.02$ for SLES and Triton X-100 after 20 days due to the difference in density between mineral oil and 0.42 M sodium chloride.

For non-pre-mixed emulsions,

- Sub-micron oil droplets were not present at any S/O for emulsions with 0% air. The oil drop size decreased with increasing surfactant concentration due to reduced interfacial tension between oil and water.
- A bulk oil drop and sub-micron oil droplets were present in emulsions with 70% air at a $S/O \leq 0.02$ for both surfactants due to splashing. Above a S/O of 0.02, the oil drop size increased with increasing surfactant concentration due to depletion flocculation of surfactant micelles.
- After 10 days of dynamic ageing, a uniform drop size distribution was formed in emulsions with a S/O of 0.2 for SLES.

Overall, it is likely that sub-micron oil droplets are already present in bilgewater prior to filtration. Therefore, the data from pre-mixed emulsions should be considered for bilgewater applications. These results show that the energy of dynamic ageing is sufficient for emulsification once a minimum surfactant concentration is reached regardless of the volume of emulsion stored in the tanks. Thus, the best way to mitigate stable bilgewater emulsion formation is by reducing surfactant concentration.

4. CONCLUSIONS AND FUTURE PERSPECTIVES

4.1 Conclusions and Implications of Results

Emulsion stability against coalescence for model bilgewater systems depends on the surfactant type, surfactant concentration, and ageing conditions. For both static and dynamic ageing conditions, SLES stabilized oil drops at a lower concentration than Triton X-100 (**Figure 2.5**, **Figure 2.9**, **Figure 2.12**). This behavior is due to a higher surface concentration for SLES and 0.42 M NaCl, to which more surfactant molecules can pack at the oil-water interface to prevent coalescence (**Table 2.1**). However, if the Triton X-100 concentration was large enough, coalescence was hindered just as effectively as SLES and salt. For statically aged emulsions, coalescence was observed for surfactant concentrations < 10 ppm SLES and < 100 ppm Triton X-100 (**Figure 2.5**). Dynamic ageing encouraged coalescence at surfactant concentrations ≤ 100 ppm and drop break up at ≥ 500 ppm for both SLES and Triton X-100 (**Figure 2.9**, **Figure 2.12**). Thus, the energy added due to ship rocking alters the minimum amount of surfactant required to make a thermodynamically stable emulsion. These results show that the movement of bilgewater during storage affects the stability of O/W emulsions and can aid or convolute oil filtration.

Originally, eliminating sloshing during dynamic ageing was thought to prevent further emulsification and produce stability similar to statically aged emulsions. However, even after removing the air from the ageing vial, sub-micron drops were formed during dynamic ageing for > 100 ppm SLES and Triton X-100 due to density differences between mineral oil and saltwater (**Figure 3.4**). **Figure 3.8** and **Figure 3.9** show that dynamic ageing can disperse mineral oil into surfactant and salt solutions without prior emulsification, regardless of the amount of air within the ageing vial.

Overall, the work presented in this document shows that once a minimum surfactant concentration is reached, emulsification due to dynamic ageing is inevitable. Therefore, the most practical way to support oil filtration of bilgewater is to lower the surfactant concentration.

4.2 Future Perspectives

The effect of dynamic ageing on the emulsification of model bilgewater emulsions has not been studied. Therefore, future investigations are vast. Since mitigating sloshing during dynamic ageing did not entirely prevent emulsification, another technique could be employed that involves adding a large volume of oil on the surface of a pre-existing emulsion and subjecting it to dynamic ageing. Onboard, a layer of oil is usually present at the surface of the bilgewater. Therefore, the proposed system would represent the physical composition of bilgewater and provide another mechanism to dampen the sloshing imparted by ship rocking. Overall, efforts to lower the energy density during dynamic ageing or ship rocking are necessary to understand the physical and chemical properties of model bilgewater emulsions and provide potential solutions to aid in oil filtration.

Although the investigation of dynamic ageing on emulsion stability for non-pre-mixed emulsions is not representative of bilgewater, the production of unimodal oil drops via dynamic ageing may benefit other applications. Therefore, one could consider exploring other physical and chemical conditions in which a unimodal drop distribution is produced via dynamic ageing.

APPENDIX A. SUPPORTING INFORMATION FROM CHAPTER 2

Energy Density of Emulsions Prepared via High Shear Mixing

The energy density provided by high shear mixing is described by the following equation.

$$E_D = \frac{P_o \rho N^3 D^5 t}{V} \quad (A1)$$

This energy depends on the power number (P_o)¹⁻³, density of the fluid (ρ), rotation speed (N), diameter of the mixer (D), emulsification time (t), and emulsion volume (V).

Derivation of Energy Density for Dynamic Aging

An energy balance between potential energy and kinetic energy can be derived for a falling object as:

$$mgh \sin \theta = \frac{1}{2} mv^2 \quad (A2)$$

Where θ is the tilt angle (see **Figure 2.1**), and h is the height, or the distance in which that object falls. Solve for the velocity to find:

$$v_{final} = \sqrt{2gh \sin \theta} \quad (A3)$$

Where the kinetic energy is:

$$KE_{final} = \frac{1}{2} m(v_{final})^2 \quad (A4)$$

An equation for energy density is related to the kinetic energy of the emulsion, the RPM of the rocker, the ageing time, and the volume of the emulsion.

$$E_D = \frac{KE_{final} * RPM * t}{30 * V_E} = \frac{m(v_{final})^2 * RPM * t}{30 * V_E} \quad (A5)$$

Substitute mass and volume terms for the density of the emulsion:

$$\frac{m}{V_E} = \rho_E = (\phi_{oil} * \rho_{oil}) + (1 - \phi_{oil})\rho_{water} \quad (A6)$$

Where ϕ_{oil} is the dispersed phase volume fraction. The energy density for dynamic ageing can be calculated by knowing the density of the emulsion, the falling height of the emulsion, the tilt angle and speed of the rocker, and the ageing time:

$$E_D = \frac{\rho_E * (gh \sin \theta) * RPM * t}{30} \quad (A7)$$

REFERENCES

- [1] D. J. McClements, “Critical review of techniques and methodologies for characterization of emulsion stability,” *Crit. Rev. Food Sci. Nutr.*, vol. 47, no. 7, pp. 611–649, 2007.
- [2] J. Coca-Prados and G. Gutiérrez-Cervelló, “Economic sustainability and environmental protection in mediterranean countries through clean manufacturing methods,” *NATO Sci. Peace Secur. Ser. C Environ. Secur.*, vol. 119, 2013.
- [3] C. McLaughlin, D. Falatko, R. Danesi, and R. Albert, “Characterizing shipboard bilgewater effluent before and after treatment,” *Environ. Sci. Pollut. Res.*, vol. 21, no. 8, pp. 5637–5652, 2014.
- [4] R. Albert and R. Danesi, “Oily Bilgewater Separators,” *Environ. Prot.*, no. November, pp. 1–27, 2011.
- [5] S. Boehmer-Christiansen, *Estimates of Oil Entering the Marine Environment from Sea-Based Activities, Reports and Studies No. 75*, vol. 19, no. 5. 2008.
- [6] H. Eskandarloo, M. J. Selig, and A. Abbaspourrad, “In situ H₂O₂ generation for de-emulsification of fine stable bilge water emulsions,” *Chem. Eng. J.*, vol. 335, no. August 2017, pp. 434–442, 2018.
- [7] M. Cheryan and N. Rajagopalan, “Membrane processing of oily streams. Wastewater treatment and waste reduction,” *J. Memb. Sci.*, vol. 151, no. 1, pp. 13–28, 1998.
- [8] J. W. Anderson, J. M. Neff, B. A. Cox, H. E. Tatem, and G. M. Hightower, “Characteristics of dispersions and water-soluble extracts of crude and refined oils and their toxicity to estuarine crustaceans and fish,” *Mar. Biol.*, vol. 27, no. 1, pp. 75–88, 1974.
- [9] U. States and E. Protection, “Environmentally Acceptable Lubricants,” *Encycl. Lubr. Lubr.*, no. November, pp. 526–526, 2014.
- [10] J. Church, D. M. Paynter, and W. H. Lee, “In Situ Characterization of Oil-in-Water Emulsions Stabilized by Surfactant and Salt Using Microsensors,” *Langmuir*, vol. 33, no. 38, pp. 9731–9739, 2017.
- [11] N. S. Ahmed, A. M. Nassar, N. N. Zaki, and H. K. Gharieb, “Stability and rheology of heavy crude oil-in-water emulsion stabilized by an anionic-nonionic surfactant mixture,” *Pet. Sci. Technol.*, vol. 17, no. 5, pp. 553–576, 1999.

- [12] J. M. Benito, M. J. Sánchez, P. Pena, and M. A. Rodríguez, “Development of a new high porosity ceramic membrane for the treatment of bilge water,” *Desalination*, vol. 214, no. 1–3, pp. 91–101, 2007.
- [13] C. D. Eastwood, L. Armi, and J. C. Lasheras, “The breakup of immiscible fluids in turbulent flows,” *J. Fluid Mech.*, vol. 502, no. November, pp. 309–333, 2004.
- [14] J. Israelachvili, *Intermolecular and Surface Forces*. 2011.
- [15] P. Ghosh and M. Banik, “Effects of Salts Containing Mono-, Di-, and Trivalent Ions on Electrical and Rheological Properties of Oil-Water Interface in Presence of Cationic Surfactant: Importance in the Stability of Oil-in-Water Emulsions,” *J. Dispers. Sci. Technol.*, vol. 35, no. 4, pp. 471–481, 2014.
- [16] T. D. Gurkov, D. T. Dimitrova, K. G. Marinova, C. Bilke-Crause, C. Gerber, and I. B. Ivanov, “Ionic surfactants on fluid interfaces: Determination of the adsorption; Role of the salt and the type of the hydrophobic phase,” *Colloids Surfaces A Physicochem. Eng. Asp.*, vol. 261, no. 1–3, pp. 29–38, 2005.
- [17] P. Kundu, A. Agrawal, H. Mateen, and I. M. Mishra, “Stability of oil-in-water macro-emulsion with anionic surfactant: Effect of electrolytes and temperature,” *Chem. Eng. Sci.*, vol. 102, pp. 176–185, 2013.
- [18] J. Caplan, C. Newton, and D. Kelemen, “Tech-Report-Novel-OilWater-Separator.pdf.” Marine Technology, pp. 111–115, 2000.
- [19] P. S. Abbott, “The Abbott Guide to Rheology.”
- [20] J. T. Padding and A. A. Louis, “Interplay between hydrodynamic and Brownian fluctuations in sedimenting colloidal suspensions,” *Phys. Rev. E - Stat. Nonlinear, Soft Matter Phys.*, vol. 77, no. 1, 2008.
- [21] G. M. Ayoub, S. I. Lee, C. N. Mazidji, I. S. Seo, H. M. Cho, and B. Koopman, “Seawater flocculation of emulsified oil and alkaline wastewaters,” *Water Res.*, vol. 26, no. 6, pp. 817–823, 1992.
- [22] D. J. McClements, *Principles, Practicies, and Techniques*, vol. 2, no. CRC PRESS. 2005.
- [23] J. R. Hunter, *Introduction to Modern Colloid Science*. Oxford, UK, 1993.
- [24] Malvern Panalytical, “Basic principles of particle size analysis. Technical report [Application Note],” 2013.
- [25] J. R. Hunter, *Foundations of Colloid Science*, vol. 1. Oxford, UK, 1986.

- [26] S. Narayan, A. E. Metaxas, R. Bachnak, T. Neumiller, and C. S. Dutcher, “Zooming in on the role of surfactants in droplet coalescence at the macroscale and microscale,” *Curr. Opin. Colloid Interface Sci.*, vol. 50, p. 101385, 2020.
- [27] H. Egger and K. M. McGrath, “Aging of oil-in-water emulsions: The role of the oil,” *J. Colloid Interface Sci.*, vol. 299, no. 2, pp. 890–899, 2006.
- [28] N. Malassagne-Bulgarelli and K. M. McGrath, “Emulsion ageing: Effect on the dynamics of oil exchange in oil-in-water emulsions,” *Soft Matter*, vol. 9, no. 1, pp. 48–59, 2013.
- [29] C. R. Davis, C. J. Martinez, J. A. Howarter, and K. A. Erk, “Impact of Saltwater Environments on the Coalescence of Oil-in-Water Emulsions Stabilized by an Anionic Surfactant,” *ACS ES&T Water*, vol. 1, no. 8, pp. 1702–1713, 2021.
- [30] J. Church *et al.*, “Impact of Interfacial Tension and Critical Micelle Concentration on Bilgewater Oil Separation,” *J. Water Process Eng.*, vol. 39, no. October 2020, p. 101684, 2021.
- [31] Z. Li, K. Lee, T. King, M. C. Boufadel, and A. D. Venosa, “Assessment of chemical dispersant effectiveness in a wave tank under regular non-breaking and breaking wave conditions,” *Mar. Pollut. Bull.*, vol. 56, no. 5, pp. 903–912, 2008.
- [32] J. Church *et al.*, “Identification and characterization of bilgewater emulsions,” *Sci. Total Environ.*, vol. 691, pp. 981–995, 2019.
- [33] S. Tcholakova, N. D. Denkov, I. B. Ivanov, and B. Campbell, “Coalescence in β -lactoglobulin-stabilized emulsions: Effects of protein adsorption and drop size,” *Langmuir*, vol. 18, no. 23, pp. 8960–8971, 2002.
- [34] A. J. Madden and G. L. Damerell, “Coalescence frequencies in agitated liquid-liquid systems,” *AIChE J.*, vol. 8, no. 2, pp. 233–239, 1962.
- [35] A. Bak and W. Podgórska, “Investigation of drop breakage and coalescence in the liquid-liquid system with nonionic surfactants Tween 20 and Tween 80,” *Chem. Eng. Sci.*, vol. 74, pp. 181–191, 2012.
- [36] W. Burger and A. G. Corbet, “Rolling of Ships,” *Sh. Stab.*, pp. 1–16, 1966.
- [37] K. G. Marinova *et al.*, “Charging of oil-water interfaces due to spontaneous adsorption of hydroxyl ions,” *Langmuir*, vol. 12, no. 8, pp. 2045–2051, 1996.

- [38] O. D. Velev, T. D. Gurkov, S. K. Chakarova, B. I. Dimitrova, I. B. Ivanov, and R. P. Borwankar, "Experimental investigations on model emulsion systems stabilized with non-ionic surfactant blends," *Colloids Surfaces A Physicochem. Eng. Asp.*, vol. 83, no. 1, pp. 43–55, 1994.
- [39] R. R. Netz, "Water and ions at interfaces," *Curr. Opin. Colloid Interface Sci.*, vol. 9, no. 1–2, pp. 192–197, 2004.
- [40] P. Jungwirth, "Spiers Memorial Lecture: Ions at aqueous interfaces," *Faraday Discuss.*, vol. 141, pp. 9–30, 2008.
- [41] P. Walstra, "Principles of emulsion formation," *Chem. Eng. Sci.*, vol. 48, no. 2, pp. 333–349, 1993.
- [42] G. Narsimhan and P. Goel, "Drop coalescence during emulsion formation in a high-pressure homogenizer for tetradecane-in-water emulsion stabilized by sodium dodecyl sulfate," *J. Colloid Interface Sci.*, vol. 238, no. 2, pp. 420–432, 2001.
- [43] S. Abbott, "Surfactant Science : Principles and Practice," *Surfactant Sci. Princ. Pract.*, pp. 1–249, 2015.
- [44] C. Li, J. Miller, J. Wang, S. S. Koley, and J. Katz, "Size distribution and dispersion of droplets generated by impingement of breaking waves on oil slicks," *J. Geophys. Res. Ocean.*, vol. 122, pp. 7938–7957, 2017.
- [45] Y. He, P. Yazhgur, A. Salonen, and D. Langevin, "Adsorption-desorption kinetics of surfactants at liquid surfaces," *Adv. Colloid Interface Sci.*, vol. 222, pp. 377–384, 2015.
- [46] M. J. Rosen and J. T. Kunjappu, *Surfactants and Interfacial Phenomena: Fourth Edition*. 2012.
- [47] V. Kedar and S. S. Bhagwat, "Effect of salinity on the IFT between aqueous surfactant solution and crude oil," *Pet. Sci. Technol.*, vol. 36, no. 12, pp. 835–842, 2018.
- [48] J. Eastoe *et al.*, "Adsorption of ionic surfactants at the air-solution interface," *Langmuir*, vol. 16, no. 10, pp. 4511–4518, 2000.
- [49] S. M. Kirby, S. L. Anna, and L. M. Walker, "Sequential adsorption of an irreversibly adsorbed nonionic surfactant and an anionic surfactant at an oil/aqueous interface," *Langmuir*, vol. 31, no. 14, pp. 4063–4071, 2015.

- [50] S. S. Tzocheva, P. A. Kralchevsky, K. D. Danov, G. S. Georgieva, A. J. Post, and K. P. Ananthapadmanabhan, "Solubility limits and phase diagrams for fatty acids in anionic (SLES) and zwitterionic (CAPB) micellar surfactant solutions," *J. Colloid Interface Sci.*, vol. 369, no. 1, pp. 274–286, 2012.
- [51] S. Khosharay, M. Rahmanzadeh, and B. ZareNezhad, "Surface Behavior of Aqueous Solutions of Sodium Lauryl Ether Sulfate, Additives and Their Mixtures: Experimental and Modeling Study," *Int. J. Thermophys.*, vol. 41, no. 12, pp. 1–17, 2020.
- [52] S. Mohan and G. Narsimhan, "Coalescence of protein-stabilized emulsions in a high-pressure homogenizer," *J. Colloid Interface Sci.*, vol. 192, no. 1, pp. 1–15, 1997.
- [53] S. Tcholakova, N. D. Denkov, and T. Banner, "Role of surfactant type and concentration for the mean drop size during emulsification in turbulent flow," *Langmuir*, vol. 20, no. 18, pp. 7444–7458, 2004.
- [54] K. L. Mittal and R. D. Vold, "Effect of the initial concentration of emulsifying agents on the ultracentrifugal stability of oil-in-water emulsions," *J. Am. Oil Chem. Soc.*, vol. 49, no. 9, pp. 527–532, 1972.
- [55] S. Llamas *et al.*, "Adsorption of Sodium Dodecyl Sulfate at Water-Dodecane Interface in Relation to the Oil in Water Emulsion Properties," *Langmuir*, vol. 34, no. 21, pp. 5978–5989, 2018.
- [56] L. Taisne, P. Walstra, and B. Cabane, "Transfer of oil between emulsion droplets," *J. Colloid Interface Sci.*, vol. 184, no. 2, pp. 378–390, 1996.
- [57] L. Djaković, P. Dokić, P. Radivojević, I. Šefer, and V. Sovilj, "Action of emulsifiers during homogenization of o/w emulsions," *Colloid Polym. Sci.*, vol. 265, no. 11, pp. 993–1000, 1987.
- [58] E. Amstad, S. S. Datta, and D. A. Weitz, "The microfluidic post-array device: High throughput production of single emulsion drops," *Lab Chip*, vol. 14, no. 4, pp. 705–709, 2014.
- [59] M. F. Fingas, E. Huang, B. Fieldhouse, L. Wang, and J. V. Mullin, "The effect of energy, settling time and shaking time on the swirling flask dispersant apparatus," *Spill Sci. Technol. Bull.*, vol. 3, no. 4, pp. 193–194, 1996.
- [60] C. W. Pouton, "Self-emulsifying drug delivery systems: assessment of the efficiency of emulsification," *Int. J. Pharm.*, vol. 27, no. 2–3, pp. 335–348, 1985.

- [61] A. Nandi, D. V. Khakhar, and A. Mehra, "Coalescence in surfactant-stabilized emulsions subjected to shear flow," *Langmuir*, vol. 17, no. 9, pp. 2647–2655, 2001.
- [62] S. Wang, W. Qin, and Y. Dai, "Separation of oil phase from dilute oil/water emulsion in confined space apparatus," *Chinese J. Chem. Eng.*, vol. 20, no. 2, pp. 239–245, 2012.
- [63] J. M. Shaw, "A microscopic view of oil slick break-up and emulsion formation in breaking waves," *Spill Sci. Technol. Bull.*, vol. 8, no. 5–6, pp. 491–501, 2003.
- [64] I. D. Nissanka and P. D. Yapa, "Oil slicks on water surface: Breakup, coalescence, and droplet formation under breaking waves," *Mar. Pollut. Bull.*, vol. 114, no. 1, pp. 480–493, 2017.
- [65] M. Li and C. Garrett, "The relationship between oil droplet size and upper ocean turbulence," *Mar. Pollut. Bull.*, vol. 36, no. 12, pp. 961–970, 1998.
- [66] Z. Chen, C. S. Zhan, and K. Lee, "Formation and vertical mixing of oil droplets resulting from oil slick under breaking waves-A modeling study," *Environ. Forensics*, vol. 10, no. 4, pp. 347–353, 2009.
- [67] K. J. Myers, M. F. Reeder, and D. Ryan, "Power draw of a high-shear homogenizer," *Can. J. Chem. Eng.*, vol. 79, no. 1, pp. 94–99, 2001.
- [68] A. J. Kowalski, "An expression for the power consumption of in-line rotor-stator devices," *Chem. Eng. Process. Process Intensif.*, vol. 48, no. 1, pp. 581–585, 2009.
- [69] J. Zhang, S. Xu, and W. Li, "High shear mixers: A review of typical applications and studies on power draw, flow pattern, energy dissipation and transfer properties," *Chem. Eng. Process. Process Intensif.*, vol. 57–58, no. October 2017, pp. 25–41, 2012.

VITA

Twenty-four years ago, Rina G. Sabatello was born in Palatine, Illinois to Rick and Tina. She received a Bachelor of Science in Materials Engineering in May of 2020. Rina's undergraduate research focused on the stability and formation of emulsions and was performed under the direction of Professor Carlos Martinez. Rina continued this research as she began her Masters in the School of Materials Engineering at Purdue University. Rina's passion for cosmetics inspired her to join the Masters in Cosmetic Science program at the University of Cincinnati. Rina hopes to pursue a career in the cosmetic industry and improve the quality of personal care products by applying the knowledge she gained at Purdue University.